GRID MODERNIZATION LABORATORY CONSORTIUM
U.S. Department of Energy

Impacts of Using Distributed Energy Resources to Reduce Peak Loads in Vermont

November 2017

Mark Ruth, Monte Lunacek, and Birk Jones

DOE/GO-102017-5057

DOE/GO-102017-5057

Impacts of Using Distributed Energy Resources to Reduce Peak Loads in Vermont

Mark Ruth[1] Monte Lunacek[1]
Birk Jones[2]

November 2017

[1] National Renewable Energy Laboratory
[2] Sandia National Laboratories

Summary

To help the United States develop a modern electricity grid that provides reliable power from multiple resources as well as resiliency under extreme conditions, the U.S. Department of Energy (DOE) is leading the Grid Modernization Initiative (GMI) to help shape the future of the nation's grid. Under the GMI, DOE funded the Vermont Regional Initiative project to provide the technical support and analysis to utilities that need to mitigate possible impacts of increasing renewable generation required by statewide goals. Advanced control of distributed energy resources (DER) can both support higher penetrations of renewable energy by balancing controllable loads to wind and photovoltaic (PV) solar generation, and reduce peak demand by shedding noncritical loads. This work focuses on the latter.

This document reports on an experiment that evaluated and quantified the potential benefits and impacts of reducing the peak load through demand response (DR) using centrally controllable electric water heaters (EWHs) and batteries on two Green Mountain Power (GMP) feeders. The experiment simulated various hypothetical scenarios that varied the number of controllable EWHs, the amount of distributed PV systems, and the number of distributed residential batteries. The control schemes were designed with several objectives. For the first objective, the primary simulations focused on reducing the load during the independent system operator (ISO) peak when capacity charges were the primary concern. The second objective was to mitigate DR rebound to avoid new peak loads and high ramp rates. The final objective was to minimize customers' discomfort, which is defined by the lack of hot water when it is needed. We performed the simulations using the National Renewable Energy Laboratory's (NREL's) Integrated Energy System Model (IESM) because it can simulate both electric power distribution feeder and appliance end use performance and it includes the ability to simulate multiple control strategies.

Two control schemes were tested: single bucket and smooth. In the single bucket scheme, all the EWHs were turned off and on simultaneously. This approach resulted in significant load rebounds and voltage sags on the feeder. To avoid the DR rebound effect, we developed and tested an alternative – the smooth control scheme. Under it, all EWHs were turned off simultaneously but returned to service sequentially over 2-3 hours to reduce the magnitude of load rebounds and voltage sags. The two control strategies were tested under several different penetrations of controllable EWHs: 0% (to set a baseline), 6% (to match the current penetration on the ER-G51 feeder), 25%, 50%, and 75%. In addition, we compared feeder performance with and without batteries and PV to provide a comparison of options and identify potential synergies.

The grid models implemented in the IESM were based on Cyme models of the ER-G51 and 9G2 feeders provided by GMP with residential building loads and EWH loads added. The load models were characterized based on census data from the region that defined the house size, age, and occupancy. The EWHs draw profiles were developed using a peer-reviewed hot water draw generation tool. The IESM models simulated the performance of the feeder and EWH tanks that were subjected to the centralized control of EWHs.

The centralized management of EWHs using the simplistic bucket control scheme resulted in reduced peak load on the feeder, but created a significant rebound when the EWHs were allowed to return to normal service. This tradeoff between peak reduction and the rebound was observed in the simulation results and shown in Figure 1. The rebound was improved using the smooth control scheme while maintaining the same level of peak reduction as the single-bucket approach. Under the single-bucket control scheme with 75% of the EWHs under centralized control, the rebound was observed to reach a peak of 175% higher than the original peak. The smooth control scheme mitigated that effect with no rebounds greater than 40% higher than the original peak. By reducing the size of the rebound, the smooth-

control scheme eliminated voltage dips outside of the acceptable range that were observed in the single-bucket simulations.

Figure 1 shows that the control schemes could reduce the peak load on a feeder by up to 25% and that peak load reduction on the ER-G51 feeder alone can reduce the capacity charge by up to $51,000 in a year and on the 9G2 feeder by $46,000 a year if the rebound peak is not considered. Even with high rebound loads, the capacity charge may be reduced because loads on parts of the grid other than this feeder are lower outside the 4-hour peak control event. The simulations also showed that additional mechanisms such as PV and batteries can reduce that charge more substantially.

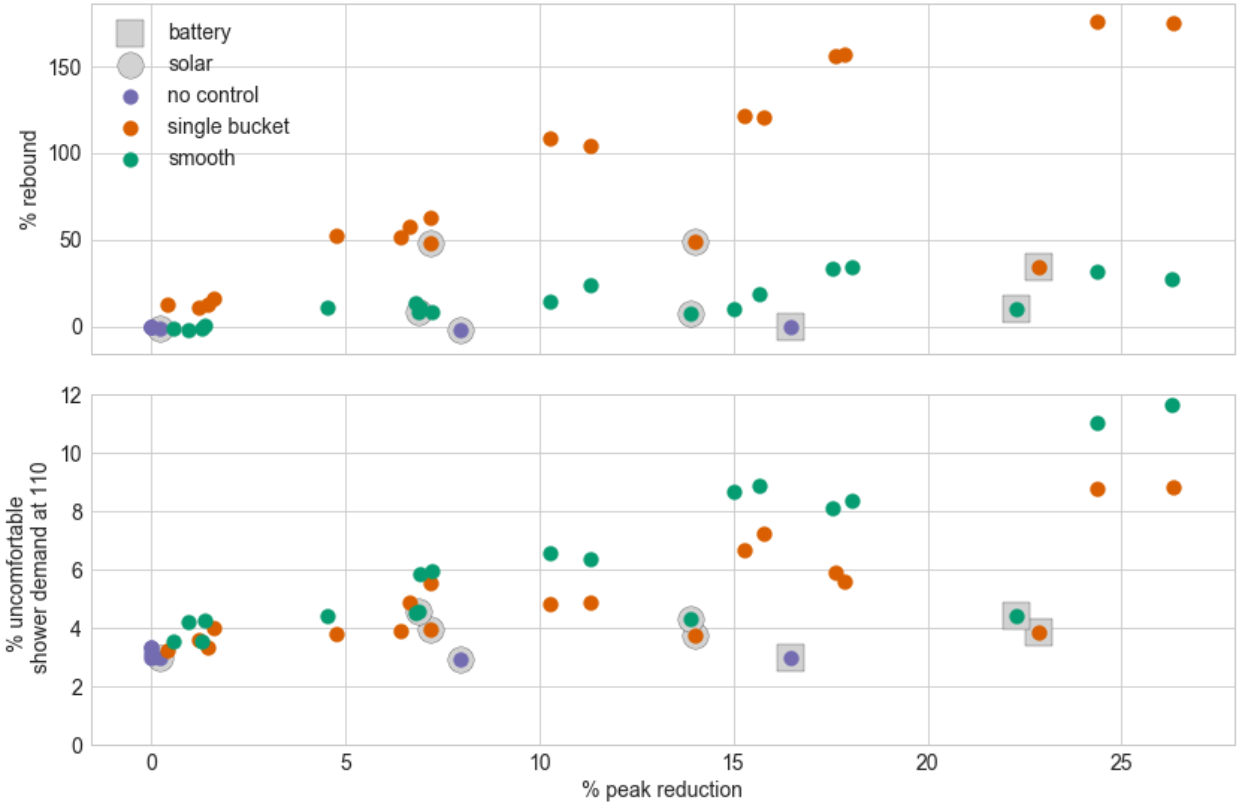

Figure 1: Peak load reductions and corresponding percent rebound (top) and percentage of uncomfortable customers (at least one minute of hot water temperature less than 110°F) in a day (bottom) for all simulations performed. Dot color indicates control scheme and outline shape indicates whether batteries or PV solar were included in simulations. Multiple seasons, feeders, and penetrations of controllable EWHs were tested.

The experiment found that, during the summer afternoon peak load events, a combination of PV solar and EWH control could reduce the peak more than either alone as long as there was sufficient solar irradiance during the peak control event; however, PV solar did not benefit the rebound as much because the rebound occurred at the same time PV generation went down due to the setting of the sun. Batteries alone could reduce the peak load by 21% during the peak load event and they did not introduce a rebound because the battery did not have to provide an immediate service and could be charged at a time that did not impact the rebound. Using both batteries and EWH control reduced the peak load by an additional 5% but introduced rebounds like those when no battery is present; however, the rebound peak for the single bucket control scheme was not as high as without a battery because the battery continued to discharge for the first hour after the peak control event – the time when the single bucket rebound peak was highest.

The experiment showed that discomfort increased with the number of controllable EWHs as shown in the bottom graph of Figure 1. In this analysis, we defined discomfort as any period when the customer required a large hot water draw (greater than 0.4 gpm for a shower or rinsing dishes) and the water temperature in the tank was below 110°F. The criteria was conservative and when applied to the baseline simulation that did not have centralized EWH DR control, approximately 3.3% of customers experience discomfort. Increasing the penetration of controllable EWHs to 75% expanded the number of customers with discomfort to over 9%. The smooth control scheme resulted in 2.5% more customers who experienced discomfort on an average day with a peak control event than under the single bucket control scheme because the EWH for some customers is out of service for longer periods of time. The increased number of customers experiencing discomfort is likely to increase the number of complaints due to a lack of hot water. However, even in the scenario where water comfort is impacted the most (75% penetration of controllable EWHs and the smooth control scheme), only 9% to 11.5% of the customers experienced at least a minute of discomfort during a day with a peak control event. Hence, 88.5%-91% of customers on the feeder will not realize they are impacted by the controls. Lower penetrations and the single bucket control scheme reduced the number of customers experiencing discomfort.

Centralized EWH control can reduce the peak load and subsequent peak charges; however, it introduces new challenges. Rebounds can lead to new peak loads, voltage control issues, and ramp rates that are costly for generation to match. Mitigating those rebounds by returning EWHs to service at a slower rate increases the number of customers experiencing discomfort and hence possible complaints. Alternative control schemes could better balance the challenges but they require additional communications such as temperatures within EWHs or the ability for the control system to interact with the EWHs at a higher frequency.

Acknowledgments

The authors acknowledge the support and assistance that we have received throughout this project. We appreciate our support from Robert Broderick (Sandia National Laboratories), the project's principal investigator, and the other project team members from Sandia especially Matt Lave and Matt Reno. We also appreciate the input and direction from the project's partners. Dan Belarmino from Green Mountain Power and Paul Hines were particularly helpful with data, information, and input. We would not have been able to accomplish what we did without building upon a number of previous efforts. The Integrated Energy System Model was developed by a team at the National Renewable Energy Laboratory (NREL) including Annabelle Pratt, Dheepak Krishnamurthy, Deepthi Vaidhynathan, and Wes Jones. We also acknowledge NREL's management and Laboratory Directed Research and Development funding who supported development of the IESM. Their effort and support are greatly appreciated. Kevin McCabe ran the domestic hot water event schedule generator and we thank him for that effort. We also thank our reviewers Annabelle Pratt, Robert Broderick, and Dave Mooney for their valuable input. Finally, we appreciate the funding and support provided by the United States Department of Energy's Grid Modernization Initiative.

Acronyms and Abbreviations

AMI	advanced metering infrastructure
ANSI	American National Standards Institute
DER	distributed Energy Resources
DR	demand response
DHWESG	domestic hot water event schedule generator
DOE	U.S. Department of Energy
EPRI	Electric Power Research Institute
ER-G51	East Rutland G51 feeder
EWH	Electric water heater
GMI	Grid Modernization Initiative
GMP	Green Mountain Power
HEMS	home energy management system
HPC	high performance computing
HVAC	heating, ventilation, and air conditioning
IESM	Integrated Energy System Model
ISO	independent system operator
NREL	National Renewable Energy Laboratory
SNL	Sandia National Laboratories
PV	photovoltaic
VRE	variable renewable energy
ZIP	load representation with constant impedance, constant current and constant power components

Contents

Figures

Tables

1.0 Introduction

To help the United States develop a modern electricity grid that provides reliable power from multiple resources as well as resiliency under extreme conditions, the U.S. Department of Energy (DOE) is leading the Grid Modernization Initiative (GMI) to help shape the future of the nation's grid. Under the GMI, DOE funded the Vermont Regional Initiative project to provide the technical support and analysis to utilities that need to mitigate possible impacts of increasing renewable generation required by statewide goals. Advanced control of distributed energy resources (DER) can both support higher penetrations of renewable energy by balancing controllable loads to wind and photovoltaic (PV) solar generation and reduce peak demand by shedding non-critical loads. This work focuses on the latter.

Vermont and its electric utilities have an ambitious goal of obtaining 90% of its electrical energy from renewable sources by 2050. If the utilities in Vermont do not mitigate the impacts of high penetrations of variable renewable energy (VRE), which may include voltage violations, equipment failures, thermal overloads, and safety and reliability issues, they will not meet the goal and continue to provide the reliability and resilience expected by customers. The core objective of the GMI's Vermont Regional Initiative project is to provide the technical support and analysis needed to develop techniques to mitigate those impacts. The objective of this project is to assist Green Mountain Power (GMP) in Vermont by providing methods and analysis that can enable high PV penetration and provide essential grid services such as utility-scale peak shaving, variability smoothing, and voltage control [Grid Modernization Laboratory Consortium]. This analysis is one task within the project and has a slightly different focus than the project as a whole – analyzing the opportunity to help reduce peak demand by shedding non-critical loads.

The task discussed in this document is the evaluation and quantification of the impacts of various control schemes for centrally controllable electric water heaters (EWHs) and batteries at several PV penetrations on GMP feeders. The key objectives are to manage peak load through demand response (DR) and to mitigate the DR rebound while minimizing customer discomfort. The simulations were performed on two distribution feeders: East Rutland-G51 (ER-G51) and 9G2. The feeder models were converted from the Cyme International format to the National Renewable Energy Laboratory's (NREL's) Integrated Energy System Model (IESM). The IESM allowed for the simulation of the feeders with distributed loads, generation, and storage. We used the IESM because it has co-simulation capabilities that enabled the modeling of appliances and feeder systems under various types of control strategies.

The primary objective was to test and analyze central DR control schemes that shed load during the Integrated Service Operators (ISO) peak demand using EWHs and distributed battery systems. Two control schemes were tested: single bucket and smooth. In the single bucket scheme, all the EWHs were turned off and on simultaneously which resulted in load rebounds and voltage sags on the feeder. To reduce the DR rebound effect, an alternative control scheme was tested – smooth. Under it, all controlled EWHs were turned off simultaneously but returned to service at a sequentially over 2-3 hours to reduce the magnitude of load rebounds. Results from simulations of both control schemes at various EWH, PV, and battery penetrations are reported here. In addition, we analyzed the impacts on customer hot water temperatures when the EWHs were turned off to shed load.

Section 2 of this report provides details on the simulation tool and methodology used to populate and run the simulation. It also discusses the control schemes tested. Section 3 summarizes the simulation results. Section 4 lists conclusions, and Section 5 provides some suggested future work to improve the simulation and control strategy.

2.0 Simulation Methodology and Control Schemes

2.1 The Integrated Energy System Model (IESM)

The IESM was used to perform the simulations in this analysis. It is a co-simulation framework [Ruth, Mittal] that runs on a high performance computing (HPC) platform to allow for parallel execution of controllers with feeder and load simulations. The IESM instance used for this analysis utilizes GridLAB-D to simulate the electrical distribution feeder, residential buildings, and appliances. GridLAB-D is an open-source, agent-based, quasi-steady-state time-series (QSTS) power system simulation tool developed by the Pacific Northwest National Laboratory [Chassin]. GridLAB-D includes a thermal model for houses that is dependent upon house size, insulation characteristics, and appliances within the houses. The IESM includes a methodology to populate the feeders with house and appliance objects that explicitly simulate loads on the feeder and how they vary over time.

For this analysis, explicit GridLAB-D models of EWHs, batteries, and PV systems were used. All other loads were aggregated as ZIP loads that consist of constant impedance, constant current, and constant power components. We expanded the capability of the IESM so that it could model electric hot water use at one-minute frequency in each of 1,000 homes over a two-week period (more than 20,000 data points per house). The native GridLAB-D methodology limited the total number of scheduling points for each house and could not manage the necessary magnitude of data points. NREL developed a communication methodology that allowed for the 50,000,000 messages (data, control commands, control responses) that needed to be transferred for these simulations.[1] In addition, NREL improved the performance of the GridLAB-D EWH models so that the electrical loads would update at the one-minute frequency necessary for this analysis.

2.2 Feeder and End-Use Models

For this analysis, GMP-provided feeder models were converted into a format that could be run in the IESM and were populated with loads and appliances. The aggregated feeder load in the simulation was matched to advanced metering infrastructure (AMI) data so that modeled feeder performance would be similar to expected performance of the actual feeders. This section summarizes the feeder models, population methodology, and performance validation of the models.

2.2.1 Feeder Models

GMP provided Cyme models of the ER-G51 and 9G2 feeders that were converted to GridLAB-D models. Because the current instance of the IESM is built to use GridLAB-D models, NREL developed and used a Python-based model conversion tool to convert the OpenDSS feeder models provided by Sandia National Laboratories (SNL) into GridLab-D. A representation of that method is shown in Figure 2. The tool reads .DSS files via a COM interface and then reconstructs the data into multiple classes representing power lines, line codes, transformers, voltage regulators, capacitors, loads, and PV generators [Electric Power

[1] One thousand water heaters providing a data message and a response at a 1min frequency for a 14-day simulation results in 40,320,000 messages. Approximately, 10,000,000 control signals are sent per simulation.

Research Institute]. The constructed classes were then translated into GridLab-D model.

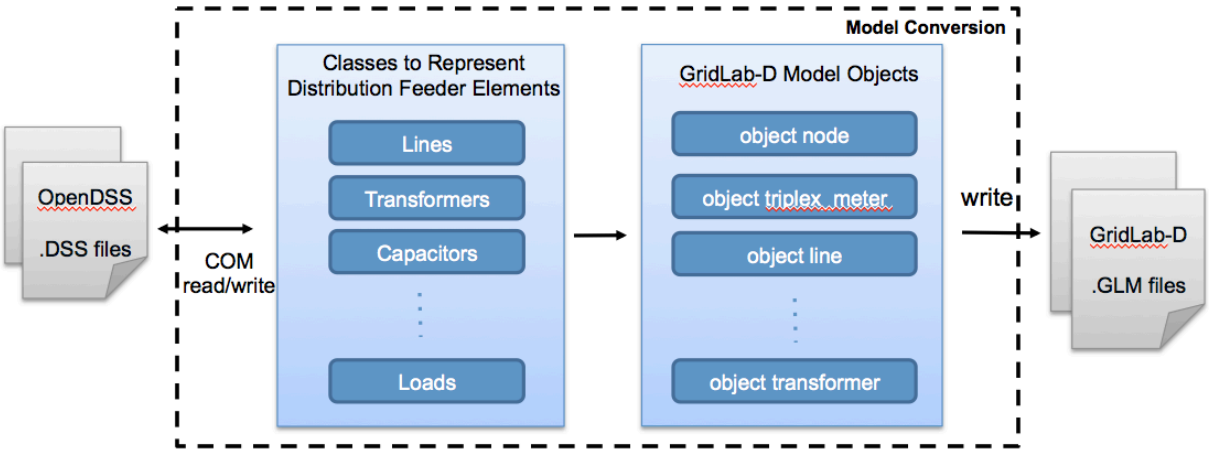

Figure 2: Representation of the method used for converting OpenDSS files to GridLAB-D files for simulations.

2.2.2 Commercial Load Estimates

Commercial loads on the feeders were represented with ZIP model loads because we did not have sufficient data to validate specific end-use models. For the IESM simulations, we used the three-phase loads defined in the Cyme model as the commercial loads in GridLAB-D and single-phase loads in the Cyme model as residential loads in GridLAB-D. We calibrated the commercial loads using the AMI data for each of the 42 three-phase loads on the ER-G51 feeder. This method was considered sufficient because, in the AMI data, the three-phase loads are only 10% of ER-G51 feeder load during the winter and summer two-week periods of the simulation. Because we did not have AMI data for the 9G2 feeder, we assumed the commercial loads make up the same fraction of the total load on the 9G2 feeder.

2.2.3 Residential Load Estimates

Residential loads are represented by specific end-use models. When the feeders were converted from Cyme models to GridLAB-D models, the loads in the Cyme model were retained. Using the IESM, we replaced the single-phase loads with house models such that one house was added for every 1,200 W of load in the Cyme model. That ratio resulted in 1,000 houses on the ER-G51 feeder, which is similar to the 988 houses reported in that feeder's AMI data. The same ratio resulted in 800 houses on the 9G2 feeder.

We set the house population to have equal portions of 2-, 3-, and 4-bedroom houses. Census data shows that 42% of the houses in Rutland, VT, have 0-2 bedrooms, 38% of the houses have 3 bedrooms, and 20% of the houses have 4-5 bedrooms [U.S. Census]. House thermal efficiency was separated in two categories: modern, relatively efficient and older, less efficient houses. The key difference between the two is the house envelope efficiency, which involves the insulation, window efficiency, and amount of infiltration. Based on census data that described 70% of the houses in East Rutland to have been built before 1980, we set 70% of the houses to be older and the remainder were modeled with modern efficiency parameters. HVAC loads were not modeled explicitly for this effort because HVAC control is outside the scope of this analysis. Hence, hot water use is the key factor for load considerations.

EWHs were modeled explicitly in each house using the single-zone EWH model available in GridLAB-D. All EWH tanks were assumed to have an 80-gal volume and a 5-degree F thermostat deadband. The

80-gal volume tank was based on the GMP recommendation described in the Rate 3 Off-Peak Water Heating Service tariff. [Green Mountain Power]. We set the EWH setpoints to 120°F, 130°F, and 140°F with one-third of the population having each set point. Setpoints were randomly distributed so they were not correlated to house size or whether EWHs were providing DR.

We created residential hot water use profiles using the domestic hot water event schedule generator (DHWESG). The DHWESG is an advanced spreadsheet tool that creates year-long schedules of hot water use for a population that is specific to both the location (Rutland, VT) and the size of houses [Hendron-A]. Water use profiles for each house on the feeder were developed so that all loads were unique. The start times of the resulting profiles were adjusted slightly to give the population more diversity regarding event timing (e.g., they were adjusted so that the first shower of the day is taken between 4:00 and 8:00 AM instead of between 6:00 and 7:00). Figure 3 shows the mean water demand used in this analysis for all houses during a summer day and the percentage of houses using water during each minute of that day used in the simulations. Demand peaks in the morning and evening when people are at home and using hot water.

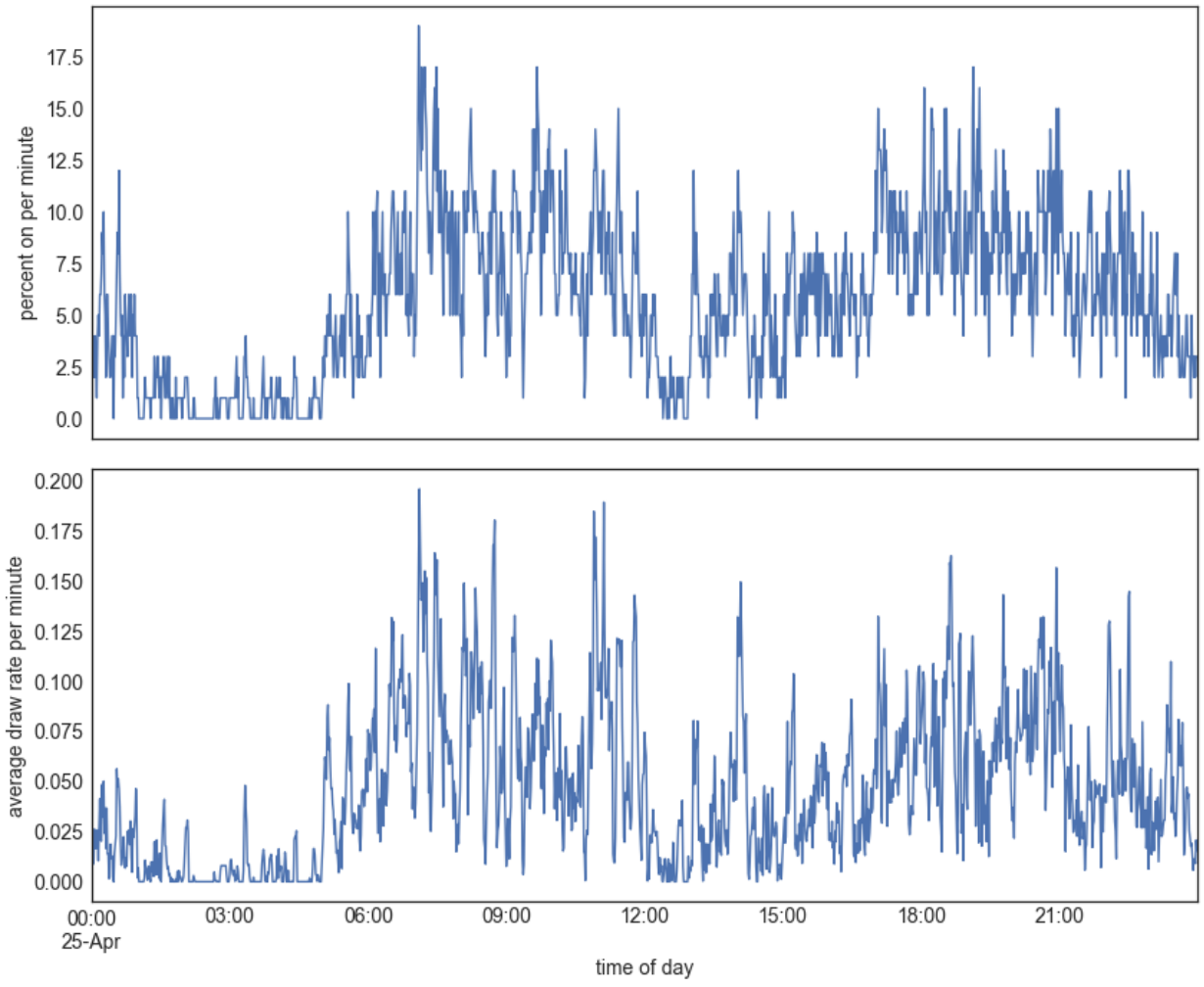

Figure 3: Average hot water draw for each minute during the day during a summer day (top) and percent of houses with water drawn during each minute (bottom).

We set the non-EWH house loads (i.e., the ZIP loads) so that the total simulated feeder load matched the load data for the full feeder. We chose that option because this project is focused on the peak power in the feeder. Since only 90 of the 1,000 houses were metered such that the EWH loads were measured separately from other household loads, we decided using the AMI data for the EWHs loads were unlikely to be representative of the full feeder. Figure 4 shows the non-EWH house load (ZIP load) from the simulations (green), the AMI data for the 90 houses that excludes EWH loads (orange), and the estimated total house load based on AMI data for the remaining 910 houses where the AMI data includes EWH loads (blue). We aimed to match the simulated average house load to the estimated average house load based on measured AMI data, and because the average simulated EWH load is bimodal, the simulated ZIP loads have the inverse shape (i.e., lower than the measured loads without the EWH in the morning and evening and higher at midday).

This methodology was used for the ER-G51 feeder in summer and winter. We used the ZIP loads developed for ER-G51 feeder in our simulations of the 9G2 feeder because AMI data for the 9G2 feeder were not available.

Figure 4: The simulated ZIP load (green) is lower in the evening than the measured load for the 90 houses that excluded EWHs (orange) because the total average load (blue) was kept the same between the simulated and measured data and the simulated EWH load has a bimodal distribution.

2.2.4 Aggregated Feeder Load Validation

Figure 5 shows average total load on the feeder during each time of day from the GridLAB-D simulation and the average of the aggregated AMI data for both summer and winter. The GridLAB-D data are the result of a two-week simulation performed using the parameters described in Sections 2.2.2 and 2.2.3. The two are similar but differ because the AMI data are based on an average over the full season and the GridLAB-D data are over the two-week simulation period. Because the two datasets are more similar than the variation between days, we considered the load estimates sufficient for the simulations used to test the control schemes.

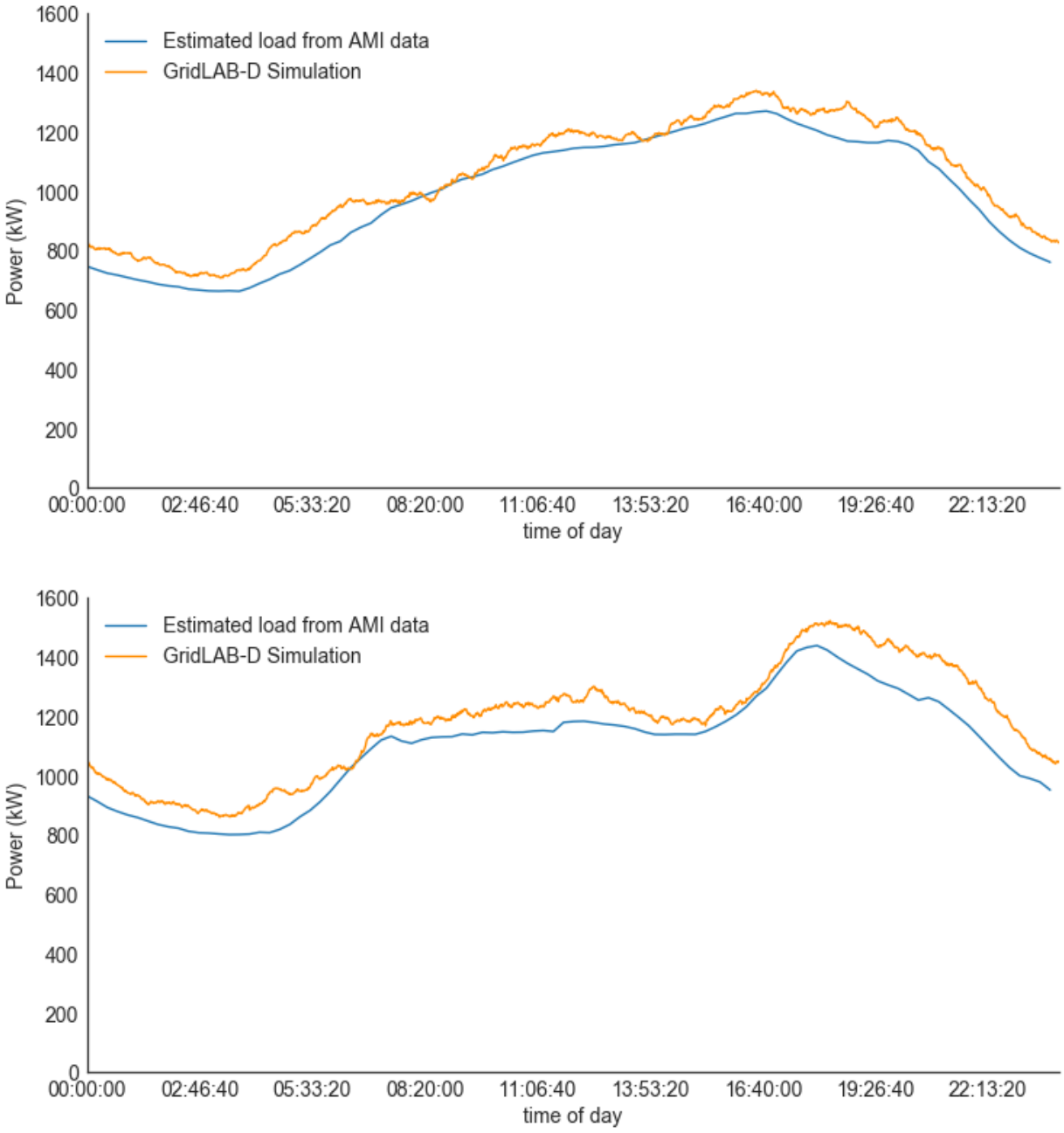

Figure 5: Without EWH control, the total load on the ER-G51 feeder approximate measured loads in the summer (top) and winter (bottom)

2.2.5 PV Solar Systems

Simulations were performed with PV arrays on 5% and 25% of the houses on each of the feeders. In these simulations, the PV systems that were approximately 2.3 kW were distributed randomly on the feeder. Each of the PV systems had an area of 150 ft2; the panels were 20% efficient, not shaded, oriented due south, and were mounted at a 45° tilt angle. We used 2015 climatological data collected at the Regional Test Center site in Williston, VT [Sandia].

2.2.6 Battery Systems

Batteries were integrated into the feeder models to test the potential benefits of using them to help manage peak loads. In those simulations, batteries were in 25% of the simulated houses distributed randomly across the feeder. All batteries had a 5,000-Wh charging capacity (i.e., they could be commonly operated to both charge and discharge 5,000 Wh each day). They had charge and discharge rates of 1,000 W. The round trip efficiencies were set to be 86%.

2.3 Length of Peak Control Events

The centralized control of distributed energy storage systems were simulated to emulate load shedding occurrences that reduced the demand during the Independent System Operator (ISO) New England (NE) peak. The simulations were used to evaluate the potential load shed amount and the associated impact on the grid as a result of controlling EWHs and battery storage systems. This evaluation was performed on two GMP feeders. Multiple simulations evaluated the impact of two control schemes for a number of different scenarios that varied the amount of controllable storage devices and the percentage of electrical generation from distributed PV systems. The control schemes depended on a load forecast to define the load-shed period.

The control schemes, tested in the present work, used the day-ahead net load forecast provided by ISO NE to estimate the hour in which the peak would occur. For example, Figure 6 shows the forecast and actual peak for July 20, 2015. The control algorithm used the forecast profile to calculate the peak and then set a load-shed period from two hours before the forecast peak to two hours after the peak so that controllable devices would be off during the actual peak. In this way, the control schemes allowed for a mismatch between the forecast and actual peak load times.

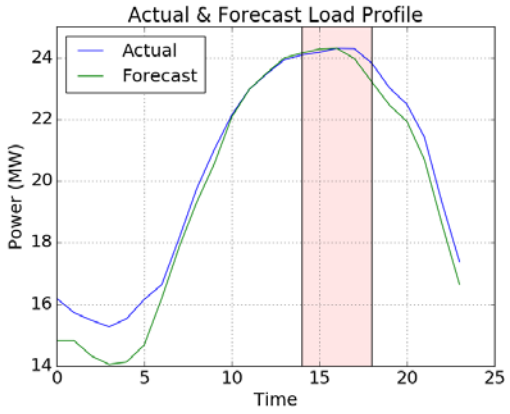

Figure 6: The peak load occurred at hour 16:00 on July 20th, 2015. The forecast accurately estimated the profile and the time of the peak, which was used by the proposed control schemes to ensure the EWHs where turned off at the time of the peak.

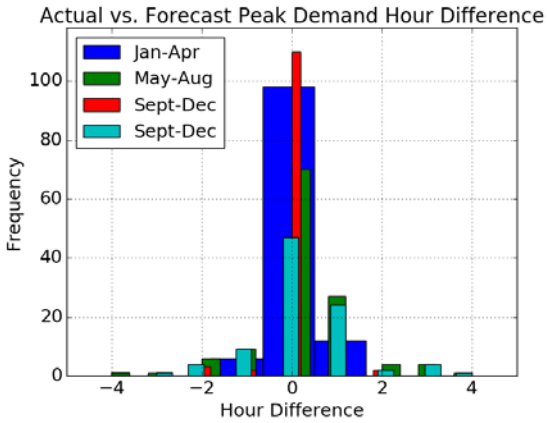

Figure 7: The frequency of the difference in hours between the actual peak time and the forecast showed a high probability that the forecast could estimate the actual peak within a range of 4 hours throughout the year.

The forecast error was defined by the difference between the actual peak hour and the estimated peak hour. The frequency at which the error occurred during different parts of the year is plotted in Figure 7. The forecast has a high probability of estimating the peak time within 4 hours of the peak (2 hours before the forecast and 2 hours after) according to data collected throughout 2015. However, there were occurrences when the forecast estimated the peak to be more than 1 hour before or after the actual peak.

The control schemes took this into account and implemented a strategy that turned off the EWHs 2 hours before and then back on 2 hours after the peak. Each of the control schemes provided a 4-hour window for the peak control event but implemented different methods for returning the EWHs back to service.

The control of distributed EWH storage devices has been implemented by GMP, which services more than 260,000 customers and controls approximately 15,000 EWHs. The EWHs are located throughout multiple feeders. The existing control scheme, deployed by GMP, splits the 15,000 EWHs into two groups. During a peak control event, GMP has typically turned off only half of the groups initially and then either 30 minutes or an hour later turns off the other half. The EWHs are returned to service in the same staggered manner. The amount of time during which the EWHs were off has been variable and ranged from 3 to 5 hours.

2.4 Control Schemes

The simulation effort tested two central EWH control schemes and their impacts on the grid and customers. Specific impacts studied include load, voltage, water temperature, customer comfort, and utility cost savings. In the single-bucket scheme, all controllable EWHs on the feeder were turned off and on simultaneously. In the smooth control scheme, all controllable EWHs were turned off simultaneously but they were returned to service at a constant rate over a 2-3 hour period after the peak control event ended. The single-bucket control scheme was designed to minimize the time the EWHs were turned off; when they all returned to service, the result was a large load rebound. The smooth control scheme reduced the rebound but resulted in some EWHs being turned off for a much longer time and, therefore, the potential impact on residents' comfort was larger. Both schemes were centrally controllable, meaning that a central control mechanism sends signals that shuts off and turns on each EWH. Participants do not have the ability to override that control signal.

The smooth control scheme was applied with varying rates at which the water heaters were returned to service. Table 1 shows the rate at which EWHs were returned to service at each penetration level of controllable EWHs on the ER-G51 feeder, and Table 2 shows the same information for the 9G2 feeder. The penetrations of controllable EWHs were chosen so that several higher penetrations could be considered and compared to the current penetration (6%). The simulations' calculation frequency was 1 minute, and EWHs could not be returned to service at a quicker rate than the calculation frequency. Therefore, we set the return to service rate for the different EWH penetrations so that the water heaters were not off for more than 3 hours. The sequence in which the EWHs are returned to services was changed randomly each day, and the control scheme was implemented so that no one home was penalized more than the others.

Table 1: Rate Used to Turn On Water Heaters under the Smooth-Control Scheme on the ER-G51 Feeder (1,000 residences served)

Number (and Percentage) of Controllable Water Heaters on the ER-G51 Feeder	Rate at Which Water Heaters were Returned to Service	Total Time to Turn on All Water Heaters
60 (6%)	1 every 3 minutes	180 minutes
250 (25%)	2 every minute	125 minutes
500 (50%)	3 every minute	167 minutes
750 (75%)	5 every minute	150 minutes

Table 2: Rate Used to Turn On Water Heaters under the Smooth-Control Scheme on the 9G2 Feeder (800 residences served)

Number (and Percentage) of Controllable Water Heaters on the 9G2 Feeder	Rate at Which Water Heaters were Returned to Service	Total Time to Turn on All Water Heaters
48 (6%)	1 every 3 minutes	144 minutes
200 (25%)	2 every minute	100 minutes
400 (50%)	3 every minute	133 minutes
600 (75%)	4 every minute	150 minutes

Returning an EWH to service did not necessarily indicate that it would start drawing power. If the EWH temperature was within the temperature deadband, it would not do so. However, due to the combination of hot water use and radiant energy losses, most EWHs in the simulation started drawing power when they are returned to service. To mitigate the immediate rebound after the peak control event, the simulation tested the potential of distributed batteries to increase the load-shed capacity and alleviate the rebound.

A battery control algorithm was added into each of the control schemes. Batteries were distributed randomly to 25% of the houses on each of the feeders. At midnight each day the batteries began charging and continued until fully charged. They started to discharge each day at the beginning of the peak control event, which was 2 hours before the forecast peak, and continued until fully discharged. Thus, they were discharging for the 4-hour peak control event each day and for 1 additional hour after the peak control event ended.

2.5 Simulations Performed

The electric feeder simulations were run over 14-day periods in summer and winter for both the ER-G51 feeder and the 9G2 feeder. Table 3 lists the controllable EWH penetrations, control schemes, PV penetrations, and battery penetrations used in simulations performed on the ER-G51 feeder, and Table 4 lists the same for the 9G2 feeder for the summer and winter seasons.

Table 3: Simulations Performed on the ER-G51 Feeder

Section	Number of Controllable Electric Water Heaters	Season	Control Schemes Simulated	PV Penetration	Battery Penetration
Standard Simulation	0	Summer and Winter	N/A	0%	0%
	60 (6%)	Summer and Winter	Single-Bucket and Smooth	0%	0%
	250 (25%)	Summer and Winter	Single-Bucket and Smooth	0%	0%
	500 (50%)	Summer and Winter	Single-Bucket and Smooth	0%	0%
	750 (75%)	Summer and Winter	Single-Bucket and Smooth	0%	0%
PV Integration Simulation	250 (25%)	Summer	Single-Bucket and Smooth	5%	0%
	250 (25%)	Summer	Single-Bucket and Smooth	25%	0%
Battery Integration Simulation	250 (25%)	Summer	Single-Bucket and Smooth	0%	25%

Table 4: Simulations Performed on the 9G2 Feeder

Number of Controllable Electric Water Heaters	Season	Control Schemes Simulated	PV Penetration	Battery Penetration
0	Summer and Winter	N/A	0%	0%
48 (6%)	Summer and Winter	Single-Bucket and Smooth	0%	0%
200 (25%)	Summer and Winter	Single-Bucket and Smooth	0%	0%
400 (50%)	Summer and Winter	Single-Bucket and Smooth	0%	0%
600 (75%)	Summer and Winter	Single-Bucket and Smooth	0%	0%

3.0 Simulation Results

The IESM models were used to simulate the feeders and loads to identify the impacts of each control scheme and compare them to each other and performance without control. The two control schemes reduced the peak load but affected grid stability by introducing rebounds at the end of the peak load event. The simulations also evaluated the impacts of PV and batteries on the peak shaving capacity and rebounds.

3.1 Peak Load Reduction Results

The primary objective of EWH control was to reduce the peak load during the peak control event period and the primary consequence was increased load when the EWHs are returned to service.

We define peak load reduction as shown in Eq.1. It is the percentage of the difference between the largest load during the control time without any controllable EWHs, batteries, or PV systems and the largest load during the control time with controllable EWHs, batteries, or PV systems with that difference divided by the largest load during the control time without any controllable EWHs, batteries, or PV systems for the same feeder and season.

$$\text{Peak Load Reduction} = \frac{P_{max_{control\ time}No\ DER\ or\ Control} - P_{max_{control\ time}With\ DER\ and/or\ Control}}{P_{max_{control\ time}No\ DER\ or\ Control}} * 100\% \quad (1)$$

We define rebound as the largest load during the rebound time (between the control time and midnight) divided by the largest load during the control time without any controllable EWHs, batteries, or PV systems for the same feeder and season minus 100% to report only the increase.

$$\text{Peak Load Reduction} = \frac{P_{max_{control\ time}No\ DER\ or\ Control} - P_{max_{control\ time}With\ DER\ and/or\ Control}}{P_{max_{control\ time}No\ DER\ or\ Control}} * 100\% \quad (2)$$

3.1.1 Standard Simulation

Standard simulations included four different penetrations of controllable EWHs; these simulations did not include batteries or PV systems. The control schemes reduced the load for 4 hours around the peak load time by shutting off the controllable EWHs during that time period. Table 5 shows the peak reduction on the ER-G51 feeder during both the summer and winter season at multiple penetrations of controllable water heaters.

Table 5: Peak Reduction Potential on the ER-G51 Feeder at Multiple Penetrations of Controllable EWHs

Penetration of Controllable EWHs	Summer Peak Reduction	Winter Peak Reduction
6%	0.4%	2%
25%	5%	7%
50%	10%	15%
75%	18%	24%

The key difference between the two control schemes was that the smooth-control scheme mitigated the rebound effect somewhat as compared to the single-bucket scheme. Figure 8 and Figure 9 show aggregated feeder loads averaged over the 2-week simulation time for the single-bucket and smooth EWH control schemes, respectively. Each figure shows multiple penetrations of controllable EWHs ranging from zero to 750. Since there are 1,000 houses on the feeder, 750 EWHs were 75% of the total resource. The forecast peak time for each day was set to the zero point on the x-axes, which then show the time before and after that point in time. Note that the y-axis for the single-bucket control scheme extends to 3,500 kW but that it only extends to 1,700 kW in the smooth-control scheme.

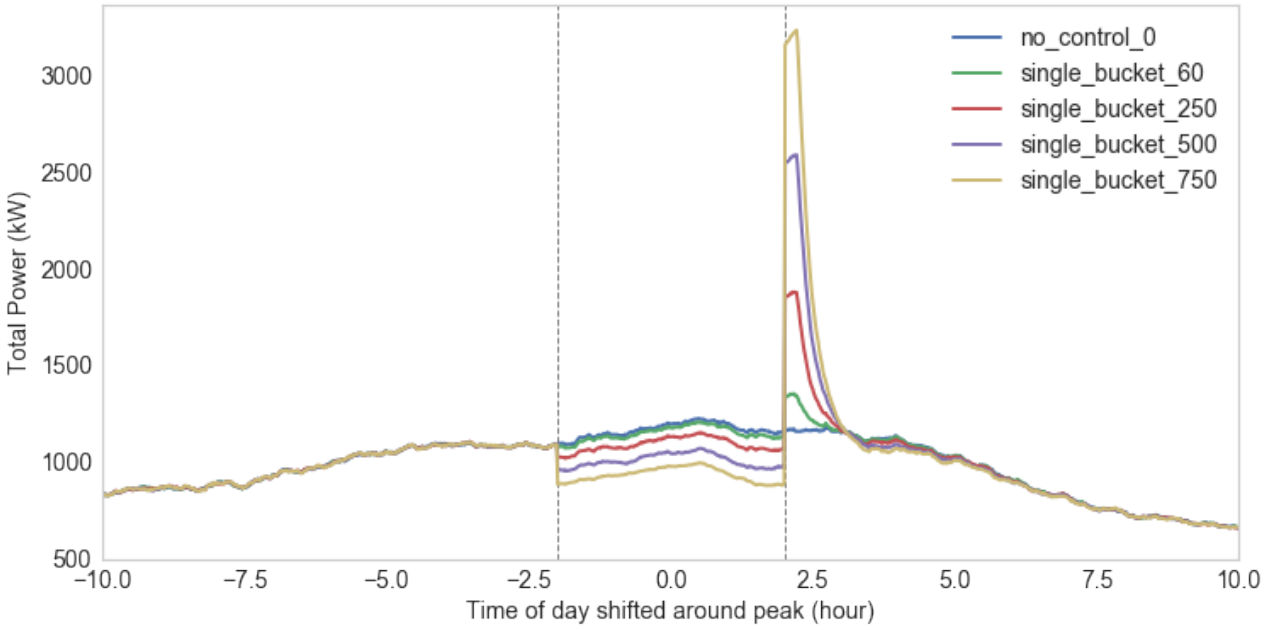

Figure 8: Load shed and rebound impacts of the single-bucket EWH control scheme at multiple penetrations of controllable EWHs on total power load for the ER-G51 feeder during the summer time period

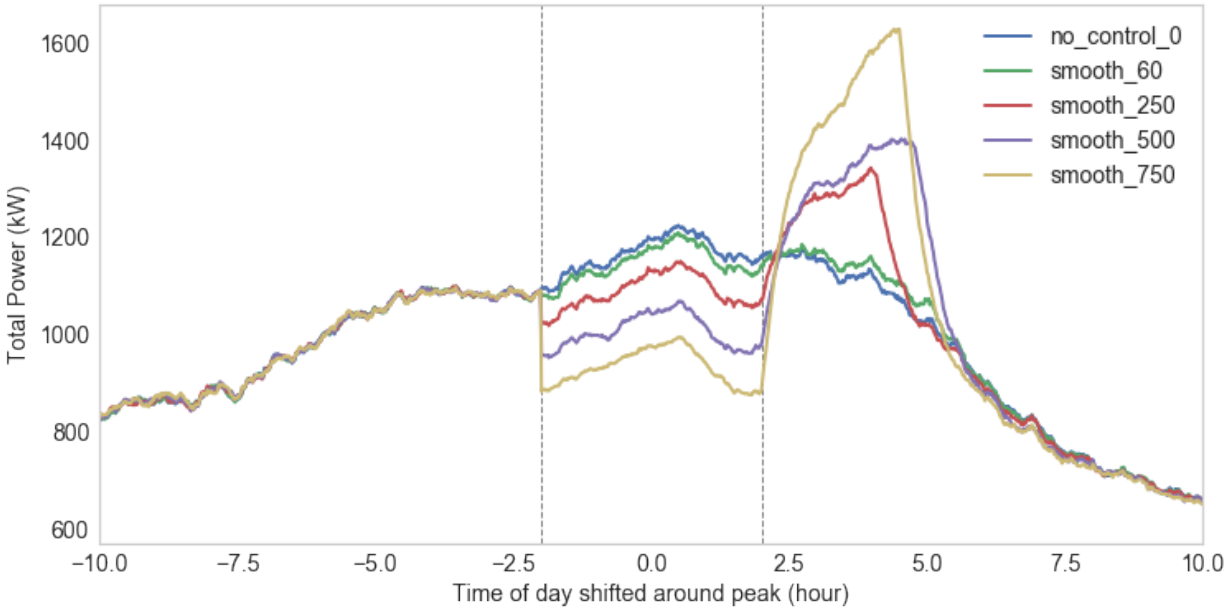

Figure 9: Load shed and rebound impacts of the smooth EWH control scheme at multiple penetrations of controllable EWHs on total power load for the ER-G51 feeder during the summer time period

Figure 10 shows a comparison of the impacts between the two control schemes–single-bucket and smooth–on total power load for the ER-G51 feeder with 750 controllable EWHs during the summer time period. Both control schemes reduce the load by 250 kW (18%) and provided relief during the ISO NE peak. However, the single bucket control scheme resulted in a rebound that increased the daily peak load from 1,400 kW to over 3,400 kW in the hour after the EWHs were returned to service. The ramp rate was also extremely high, which is likely to increase the difficulty of matching generation to the load. The smooth control scheme resulted in a longer time to return all the EWHs back to service, but the peak load only increased from 1,400 kW to 1,700 kW. As a result, the ramp rate was much lower which makes it easier to match generation to the load. Hence, the smooth control scheme is likely to simplify the generation and operational requirements to match the load.

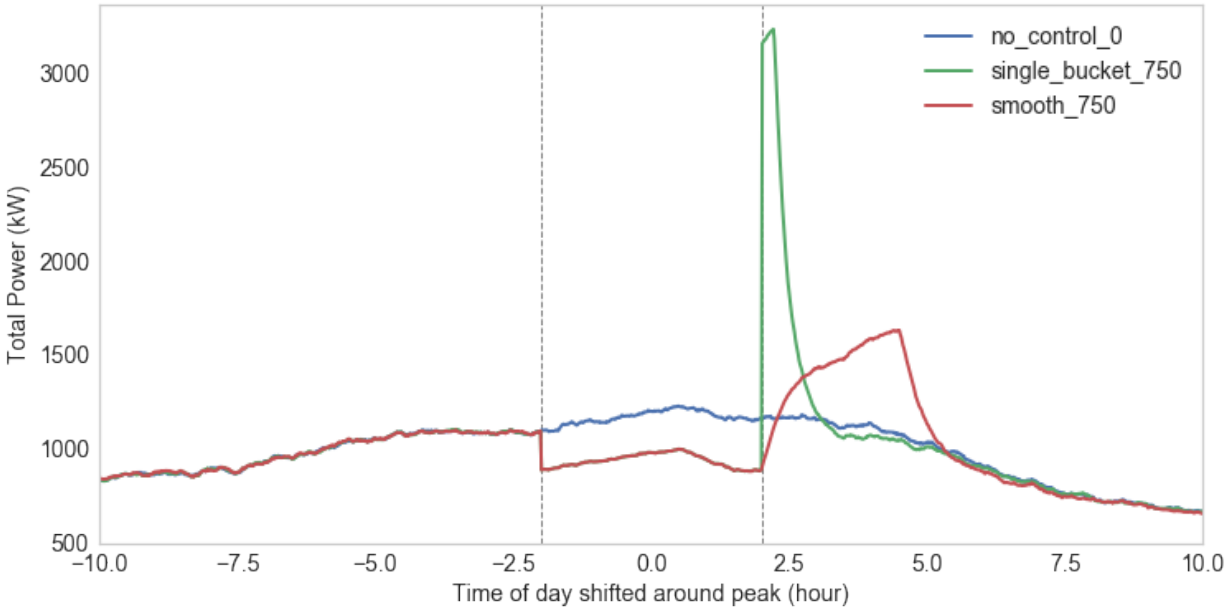

Figure 10: Comparison of the impacts of the single-bucket and smooth EWH control schemes on total power load for the ER-G51 feeder with 750 controllable EWHs during the summer time period

Table 6 shows the peak reduction potential and maximum rebounds for the single-bucket and the smooth-EWH control schemes on the ER-G51 feeder during both summer and winter. Winter peak loads are 8% higher than summer. Rebound peaks under the single-bucket control scheme are higher in both seasons; however, rebound peaks under the smooth-control scheme in winter were only somewhat higher than the original peak whereas, in the summer they are much larger. The reason is that the drop off in energy use after the peak period is greater in the winter than in the summer. The 9G2 feeder simulations show the same effects. Figure 11 and Figure 12 show the simulated loads on each feeder during both summer and winter under the single bucket and the smooth control schemes, respectively.

Table 6: Peak Reduction Potential and Rebound Impacts of Two Control Schemes on the ER-G51 Feeder at Multiple Penetrations of EWHs

	Summer			Winter		
Penetration of Controllable EWHs	**Peak Reduction**	**Maximum Rebound – Single-Bucket**	**Maximum Rebound – Smooth**	**Peak Reduction**	**Maximum Rebound – Single-Bucket**	**Maximum Rebound – Smooth**
6%	0.4%	5%	-7%	2%	6%	-8%
25%	5%	43%	4%	7%	49%	-1%
50%	10%	96%	7%	15%	103%	1%
75%	18%	140%	25%	24%	153%	21%

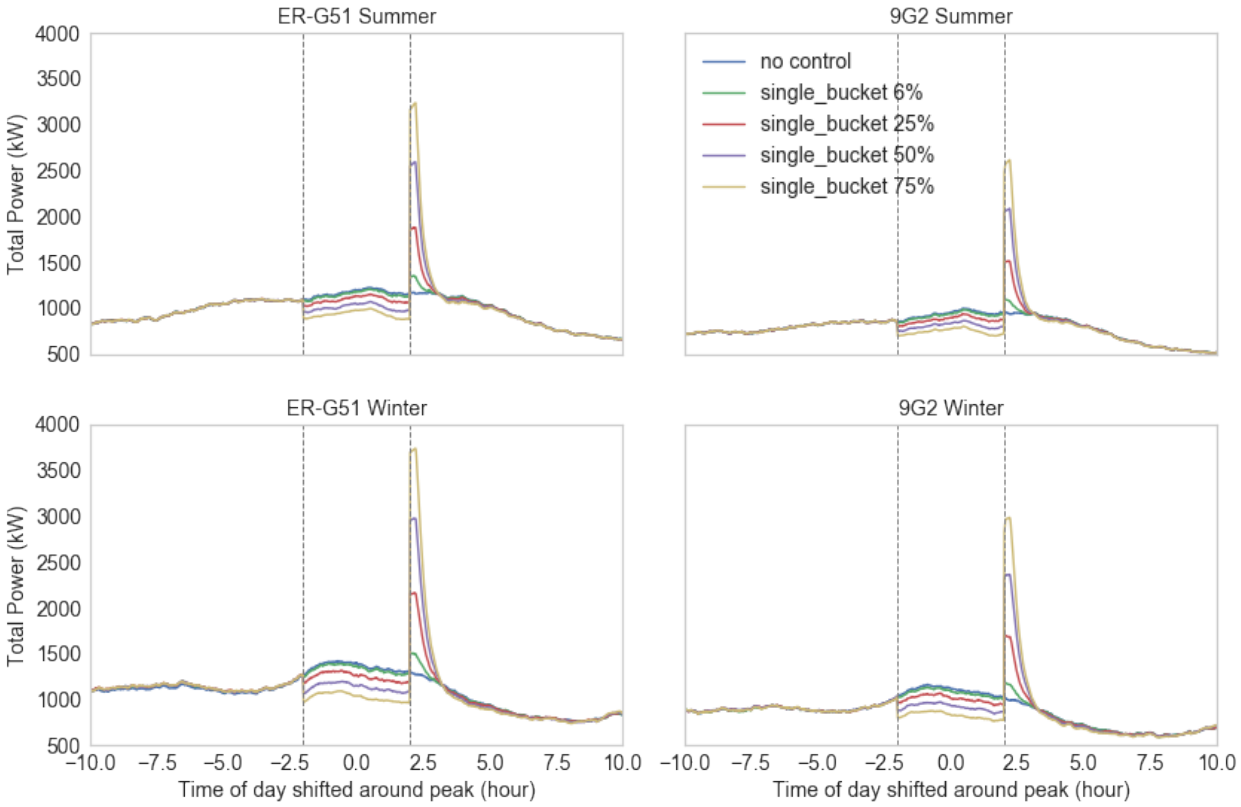

Figure 11: Comparison of the impacts of the single-bucket EWH control scheme on total power load for the ER-G51 feeder (left) and the 9G2 feeder (right) during the summer (top) and winter (bottom) time periods

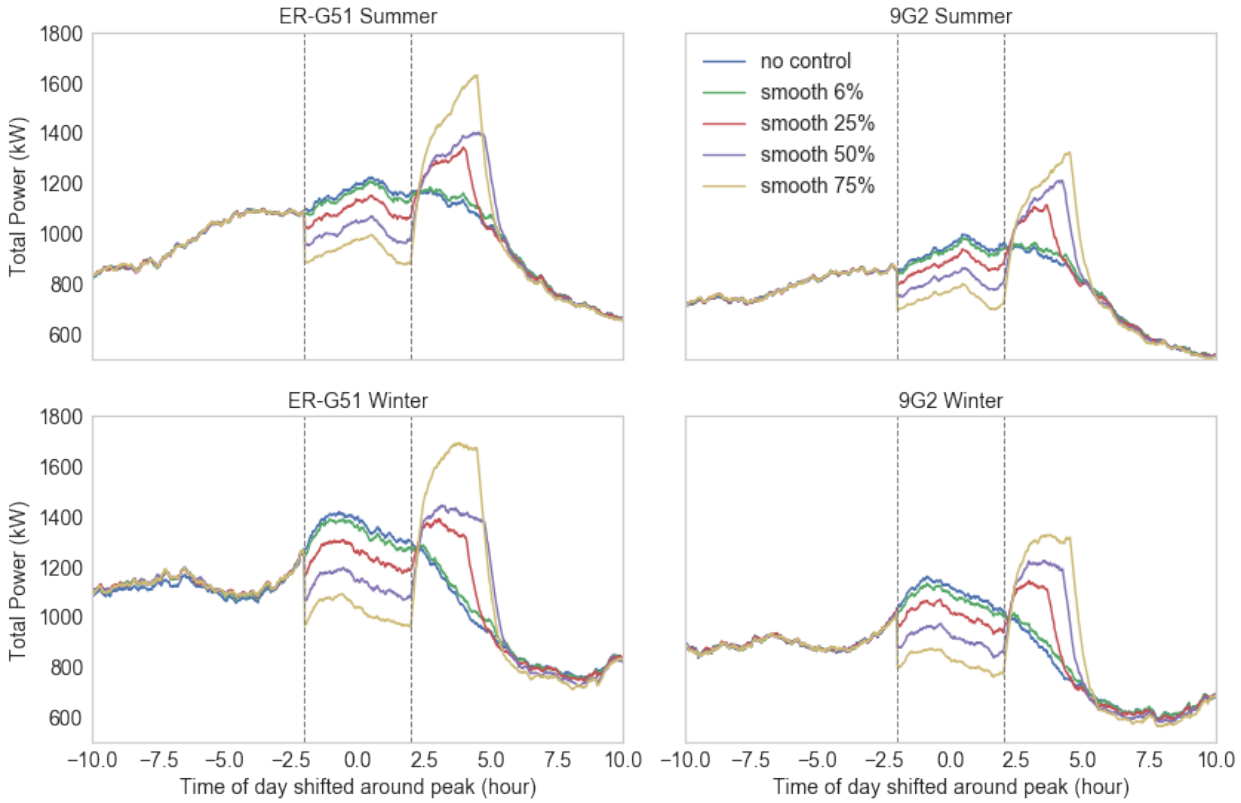

Figure 12: Comparison of the impacts of the smooth EWH control scheme on total power load for the ER-G51 feeder (left) and the 9G2 feeder (right) during the summer (top) and winter (bottom) time periods

3.1.2 PV Integration Simulation

We also tested the impact of PV on the feeder with and without peak control events where the EWHs are controlled. The integration of PV was simulated in four different scenarios that varied the number of controllable EWHs from 0 to 250, and the percentage of homes that had a solar PV system where tested at 5% and 25%.

Figure 13 shows the comparison of the different EWH control schemes for the scenario in which 5% of the homes have a 2.3-kW PV system. Figure 13 shows the load during the summer time period without PV or any controllable EWH (blue), PV on 5% of the houses and no controllable EWHs (green), PV on 5% of the houses and 25% of the houses with EWHs controlled using the single-bucket control scheme, and PV on 5% of the houses and 25% of the houses with EWHs controlled using the smooth-control scheme.

PV solar generation probably cannot be utilized to reduce peak loads because that peak reduction is dependent upon the irradiance during the peak time (at 5% PV penetration, generation at the peak time averages 33 kW on the feeder during the summer). However, over a two-week period during the summer, PV solar reduced the average peak during the key hours. With control, the peak during the control time was reduced from the non-PV scenario by 110 kW (8%). The peak rebound was not reduced by as much under either control scheme: including PV, the maximum load due to the rebound was 0.7% less for the single-bucket control scheme and 1.7% less for the smooth-control scheme than without PV because the rebound occurred at the same time as solar generation was going down due to sunset.

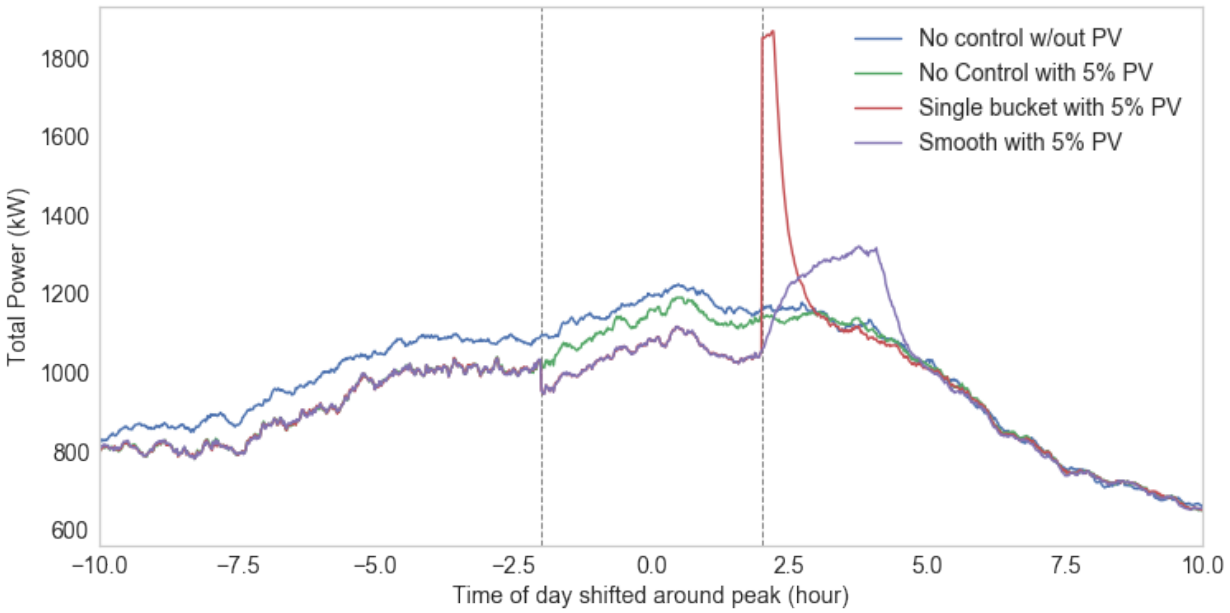

Figure 13: Comparison of the impacts of PV on 5% of the houses in conjunction with the single-bucket and smooth-EWH-control schemes on total power load for the ER-G51 feeder with 25% of the EWHs being in the summer time period

Figure 14 compares the different EWH control schemes with 25% of the homes providing electrical power from their 2.3-kW systems. The increased penetration of PV dramatically reduced the average net load during the peak control event. The reduction was 180 kW (15%) on average (with the caveat that the value was an average and the benefits of peak reduction are dependent upon irradiance at the same time as the peak control event). With control, the peak during the peak control event was reduced from the non-PV scenario by 260 kW (21%). The peak rebound was not reduced by as much under either control scheme: including PV, the maximum load due to the rebound was 6.2% less for the single-bucket control scheme and 3.2% less for the smooth-control scheme than without PV.

A combination of PV and EWH control can reduce the peak more than either alone as long as the solar irradiance is high during the peak control event; however, PV solar does not benefit the rebound as much because the rebound occurs at the same time PV generation goes down due to the setting of the sun.

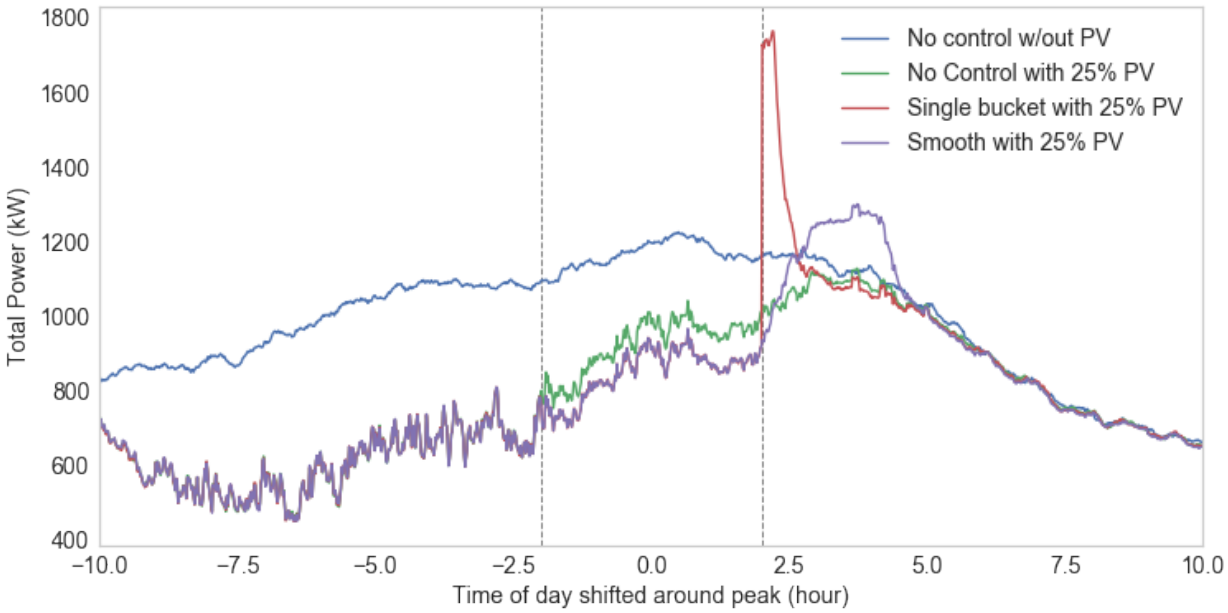

Figure 14: Comparison of the impacts of PV on 25% of the houses in conjunction with the single-bucket and smooth-EWH-control schemes on total power load for the ER-G51 feeder with 25% of the EWHs being during the summer time period

3.1.3 Battery Integration Simulation

We analyzed the impact of a 25% penetration of batteries on the ER-G51 during the summer peak control events. The battery simulations were conducted with and without a 25% penetration of controllable EWHs but no PV. Both EWH control schemes were simulated with batteries present. Figure 15 shows the results of those simulations.

Batteries alone reduced the peak load by 21% during the peak control event. The rebound they introduced is late at night when the sum of the battery charging, ZIP, and EWH loads is lower than during the day. Including the EWH, control can reduce the peak load by an additional 5% but introduces rebounds like those when no battery was present; however, the rebound peak for the single-bucket control scheme was not as high as without a battery because the battery was continuing to discharge for the first 30 minutes after the peak control event—the time when the single-bucket rebound peak was highest. A load spike occurs when batteries stop discharging at that time. A combined battery-EWH control scheme could likely be developed to better manage peak loads without introducing rebounds such as the one used in this analysis as discussed in Section 5.1.

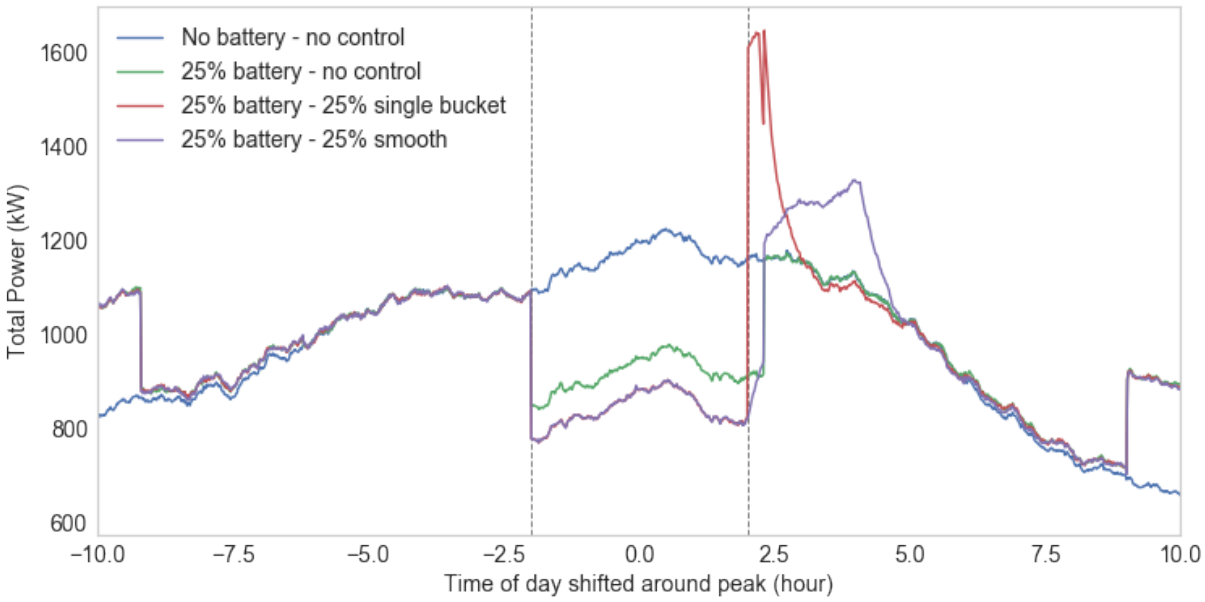

Figure 15: Comparison of the impacts of a 25% battery penetration in conjunction with the single-bucket and smooth-EWH-control schemes on total power load for the ER-G51 feeder with 25% of the EWHs during the summer time period

3.1.4 Simulation Summary

The simulation of the two control schemes showed that the load on each of the feeders can be reduced by about 18% in the summer and 25% in the winter on each of the feeders. However, the reduction in load causes a rebound when the EWH systems were allowed to return to service. The load reduction and rebound for each of the scenarios are aggregated into a single plot as shown in Figure 16. The resulting rebound was much smaller for the smooth-control scheme than for the single-bucket scheme.

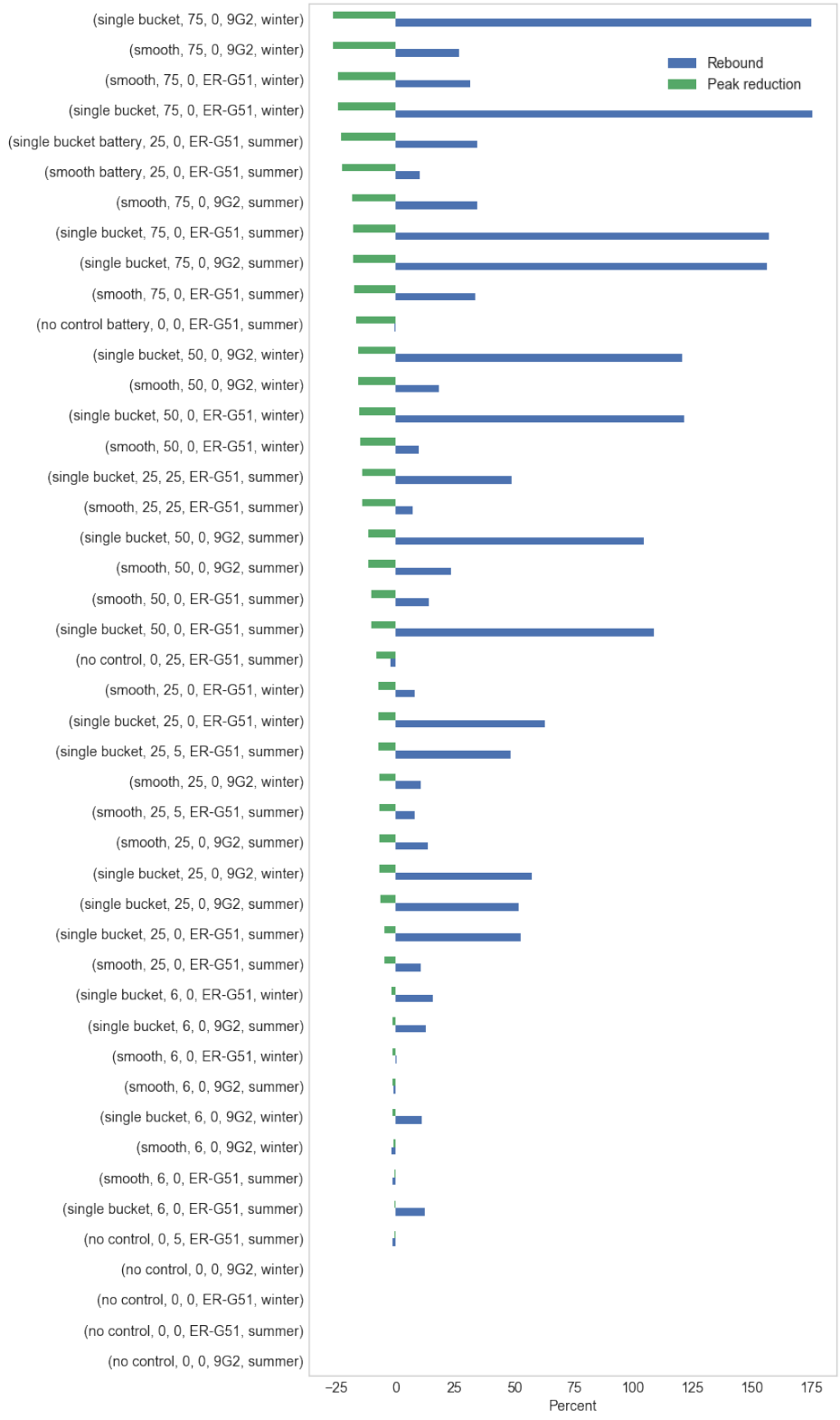

Figure 16: Comparison of the peak load reduction (green bars) and the peak increase due to the rebound (blue bars) for all scenarios. The columns in the legend indicate the EWH control scheme, presence of a battery, percentage of houses with PV, percentage of houses with controllable EWHs, feeder, and season.

Figure 17 and Figure 18 show the peak reduction and rebounds on both feeders during the summer and winter seasons. The peak load reduction was lower for both feeders during the summer than during the winter because the fraction of the load for heating water during the peak control event was smaller during the summer than the winter. Data were insufficient to know the reason; however, it could be caused by differences in inlet water temperature. Because peak times were during daylight hours, lighting and other appliances were unlikely to be too different between the seasons.

The rebound was much smaller with the smooth scheme than the single-bucket scheme as was shown in previous figures. When 6% of the EWHs were controlled, the rebound was less than the uncontrolled peak in the smooth-control scheme, whereas, it was somewhat higher than the initial peak when the single-bucket control scheme was used. The rebound increased in both control schemes. At a 25% penetration, the rebound for the smooth control scheme was less than the original peak in the winter but was more than 10% higher than the original peak in the summer. Thus, a new peak may be introduced in the summer but not in the winter at that penetration level. Throughout, the rebound with the smooth-control scheme was less than one-fourth of that with the single-bucket scheme.

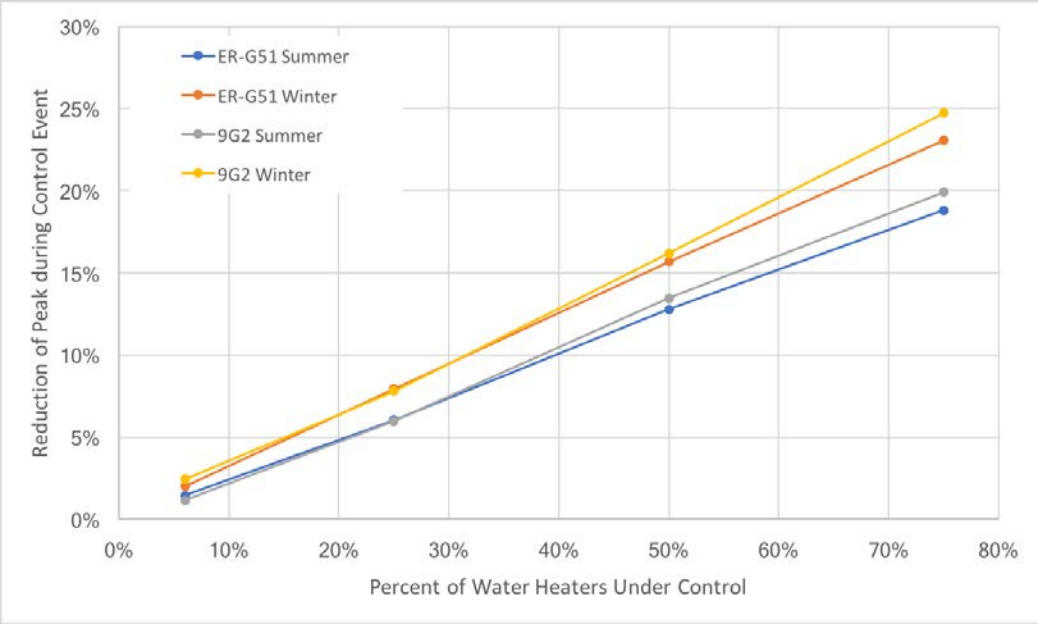

Figure 17: Reduction in peak load during the peak control event at multiple penetrations of controllable EWHs for both feeders during each season

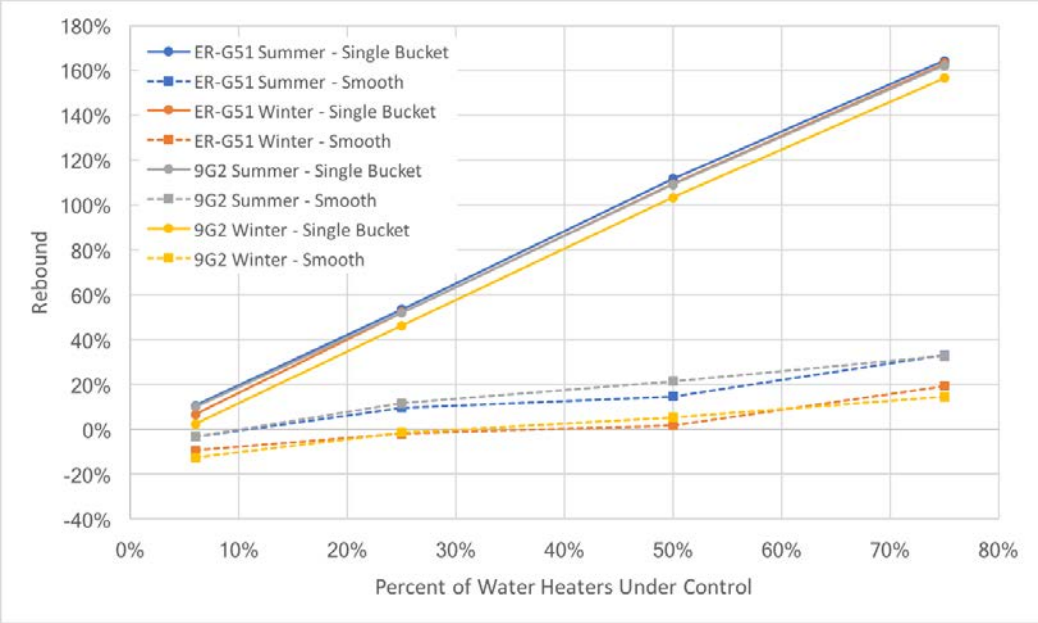

Figure 18: Peak load rebound during the peak control event at multiple penetrations of controllable EWHs for both feeders during each season

3.2 Voltage Results

Another potential impact of the control schemes on customers and the utility was feeder voltage. As shown in Figure 19, simulated voltage on the ER-G51 feeder during the summer without EWH control performed within the voltage range that the utility is expected to maintain— +/- 5% (114V to 126V). [American National Standards Institute - ANSI]. The average voltage at all the house meters during the summer time period stayed between 120 V and 122 V with a small dip in the middle of the day when the load peaked. Over 95% of the meters were at voltages above 118 V at all times and over 99% were above 117 V at all times. The minimum extreme only dips below 115 V a few times during the day and always stays above 114V.

Measured voltages were not available so the simulations were not validated.

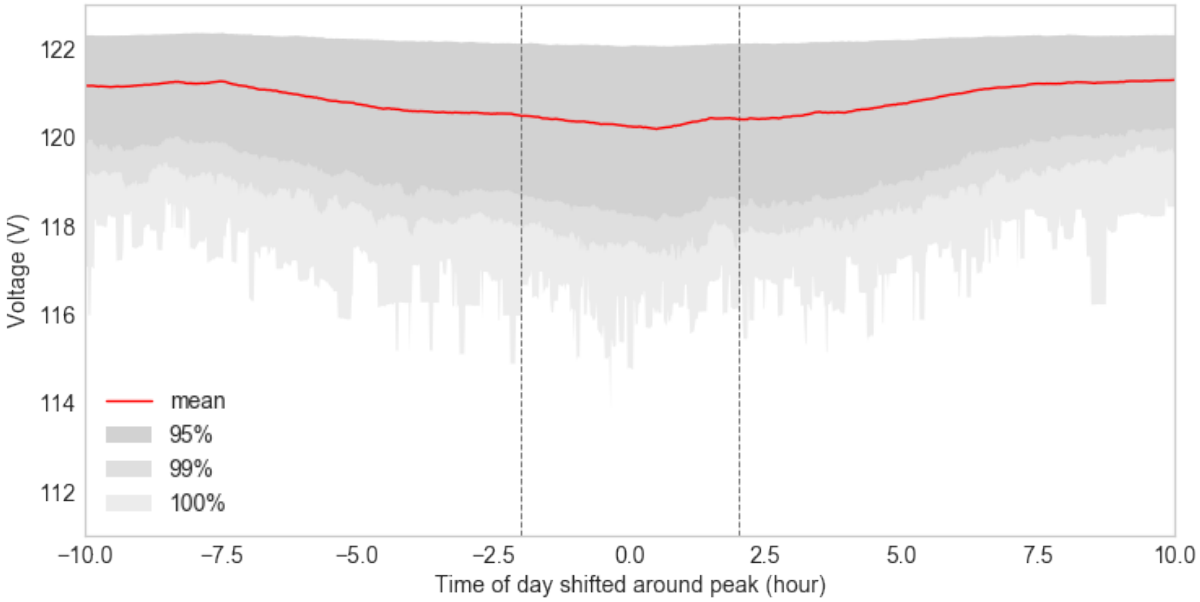

Figure 19: Voltages at house meters on the ER-G51 feeder for one-minute sampling periods during the summer time period without any control. The red line is the mean voltage, the gray area shows the range between minimum and maximum voltages with 95% of the meters falling in the darkest gray area and 99% falling in the medium and darkest gray areas.

The impacts of the single-bucket control scheme on feeder voltage are shown in Figure 20. The top, middle, and bottom images in that figure show the average, the 95% range, the 99% range and the extents of the simulated voltages for the ER-G51 feeder during the summer time period with 6%, 25%, and 75% of the EWHs under control, respectively. By returning all the EWHs to service simultaneously, the increased load resulted in sharp drops in average voltage and some meters at voltages under 114 V—outside ANSI standards. However, even at 75% penetration of controllable EWHs, about 95% of the meters were always above 114 V (5% lower than the 120 V nominal voltage).

The impacts of the smooth-control scheme on feeder voltage are shown in Figure 21. Because the controllable EWH returned to service over a 2-3 hour period, the sharp voltage drops seen in the single-bucket control scheme are not present and the voltage at almost all locations at almost all times stays above 114 V. Thus, the smooth-control scheme did not experience voltages below 114 V, as compared to the single-bucket control scheme, which resulted in times when the voltage at various meters dipped below 114 V.

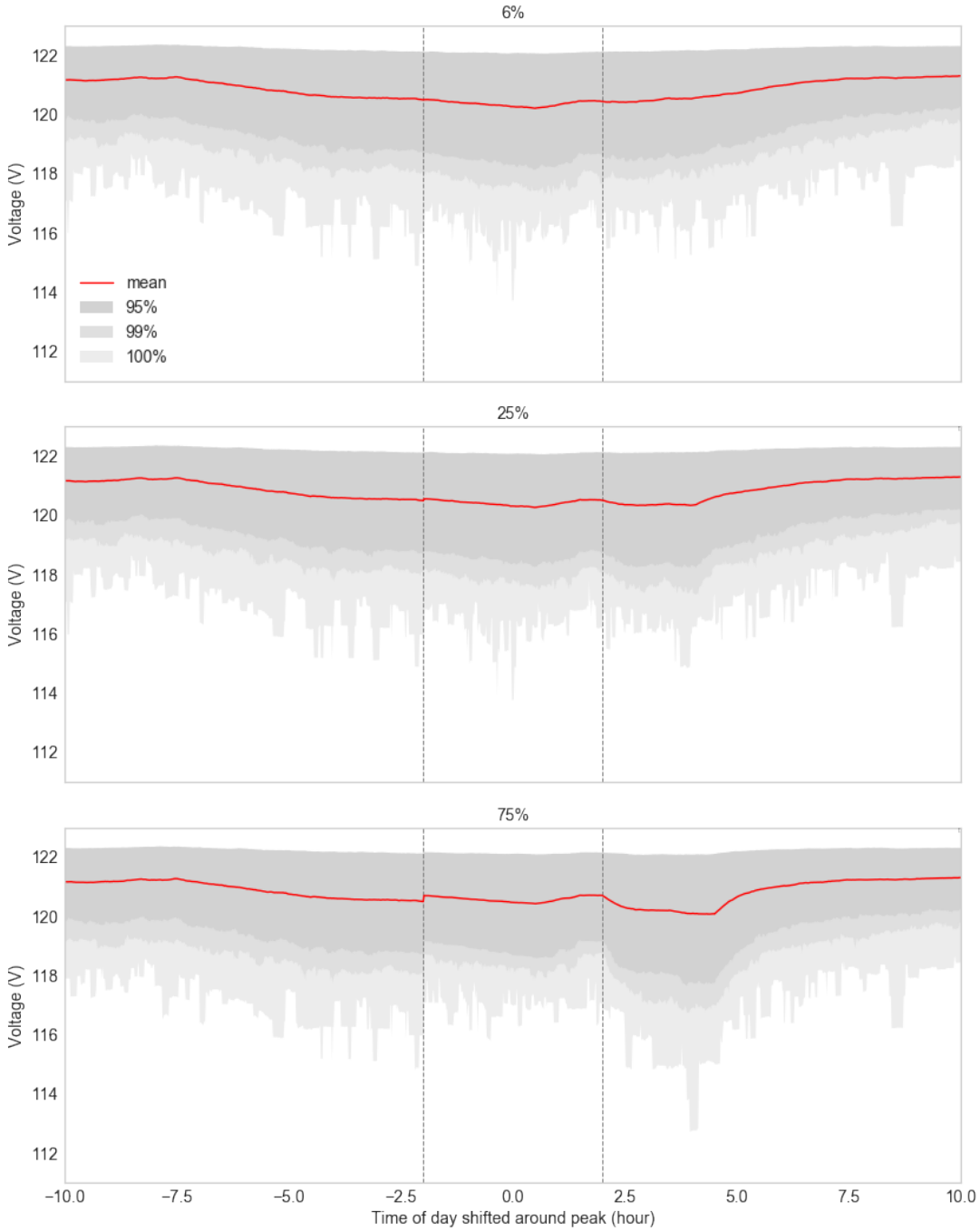

Figure 20: Feeder voltages on the ER-G51 feeder during the summer time period with single-bucket control of EWHs at various levels of controllable EWHs: 6% (top); 25% (middle); 75% (bottom). The red line is the mean voltage, the gray area shows the range between minimum and maximum voltages with 95% of the meters falling in the darkest gray area and 99% falling in the medium and darkest gray areas.

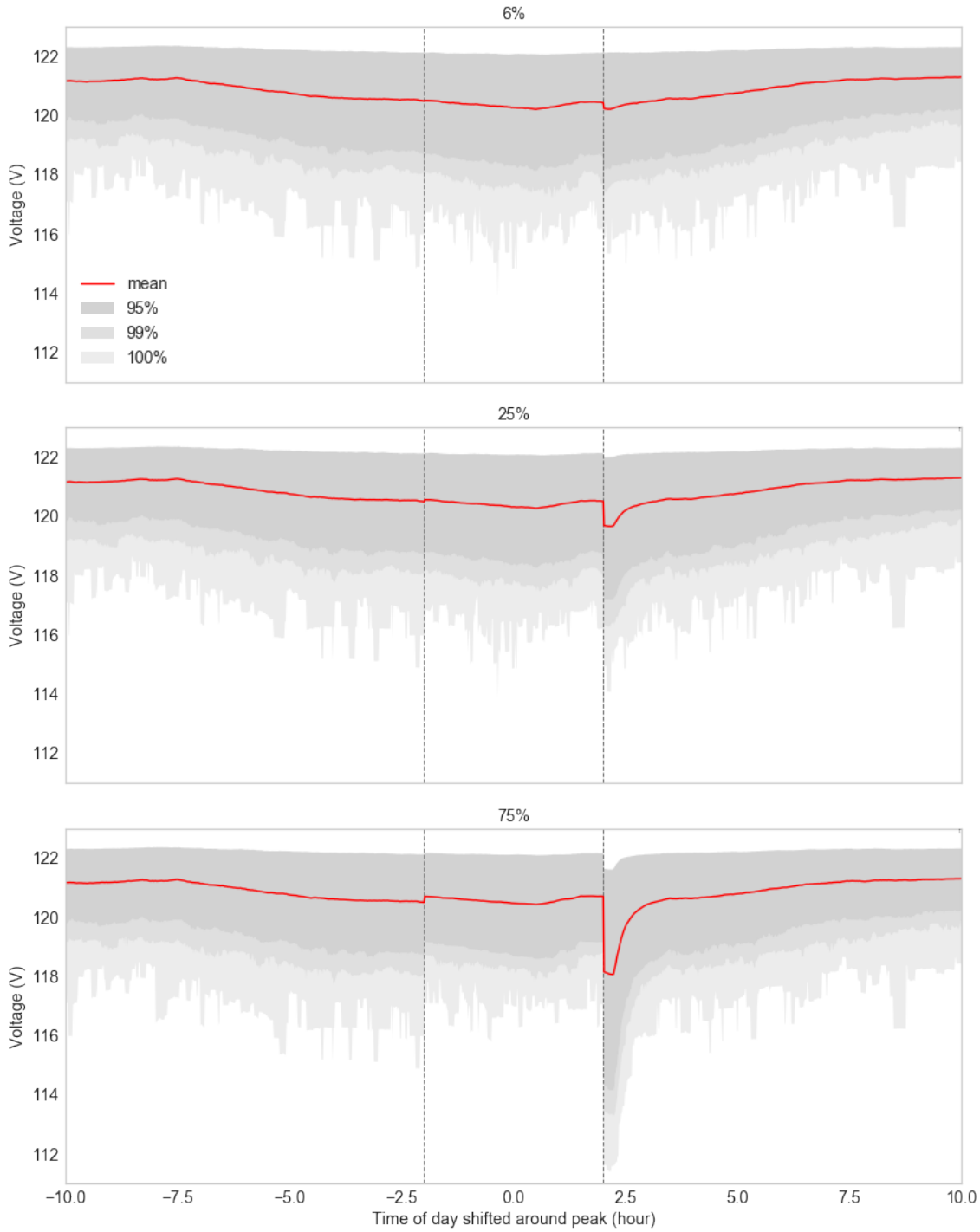

Figure 21: Feeder voltages on the ER-G51 feeder during the summer time period with smooth control of EWHs at various levels: 6% (top); 25% (middle); 75% (bottom). The red line is the mean voltage, the gray area shows the range between minimum and maximum voltages with 95% of the meters falling in the darkest gray area and 99% falling in the medium and darkest gray areas.

The ER-G51 feeder had similar performance in the winter season at each penetration of controllable EWHs. Figure 22 shows the calculated voltages on the 9G2 feeder during the summer without a control scheme managing EWHs. The simulation calculated low-voltage occurrences (below 114 V) at some meters on the feeder on a regular basis prior to the implementation of the DR control schemes. Hence, the simulation results require validation before conclusions can be made on the actual system because load characteristics were based on assumptions derived from the ER-G51 data. The voltage dips below 114 V were not verified in the actual system. If the actual houses have lower loads or there are fewer houses than the 800 we used in our simulation, the feeder is less likely to experience the voltage drops found in the simulation.

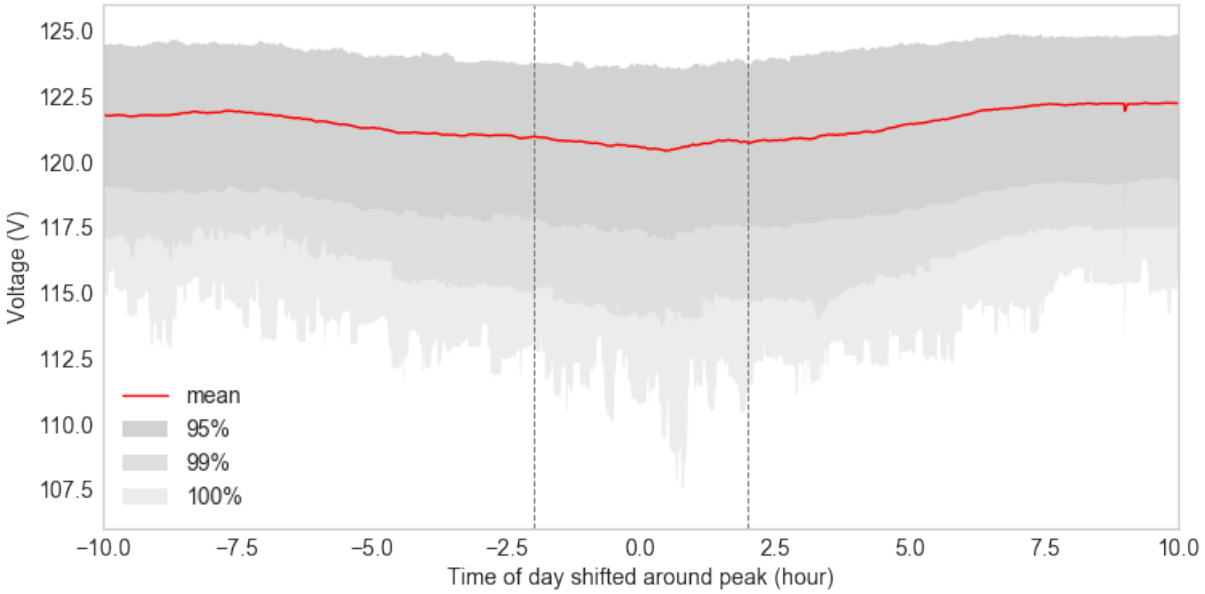

Figure 22: Feeder voltages on the 9G2 feeder during the summer time period without any control. The red line is the mean voltage, the gray area shows the range between minimum and maximum voltages with 95% of the meters falling in the darkest gray area and 99% falling in the medium and darkest gray areas.

The regularity of low voltage dips below 114 V increased with the single bucket control scheme especially at higher penetrations of controllable EWHs. Figure 23 shows those impacts during the summer time period with 6%, 25%, and 75% of the EWHs under control. At 25% and higher penetration of controllable EWHs, voltages under 114 V occurred every minute for at least an hour after the EWHs were returned to service.

When compared to the single-bucket control scheme, the smooth-control scheme reduced the magnitude of the voltage differences with the nominal voltage, but still resulted in many times when the voltage at some meters dropped below 114 V. Figure 24 shows the voltages at three penetrations of controllable EWHs under the smooth control scheme. The minimum voltage in each was the same or higher than for the single-bucket scheme but, as was found for the ER-G51 feeder, the low extreme voltages were lower than those for the single-bucket control scheme for the duration of the time window over which the EWHs were returned to service.

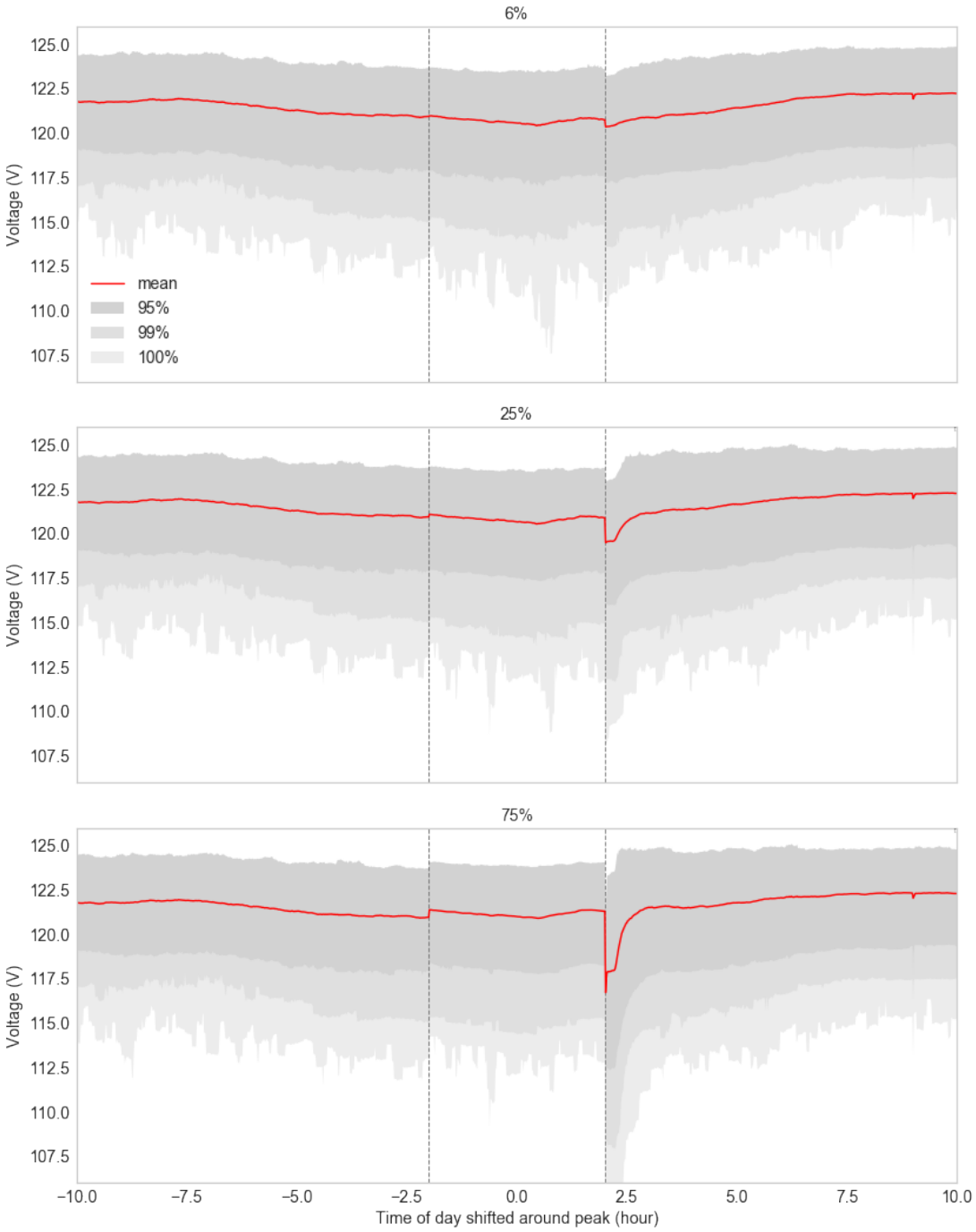

Figure 23: Feeder voltages on the 9G2 feeder during the summer time period with single-bucket control of EWHs at various levels: 6% (top); 25% (middle); 75% (bottom). The red line is the mean voltage, the gray area shows the range between minimum and maximum voltages with 95% of the meters falling in the darkest gray area and 99% falling in the medium and darkest gray areas.

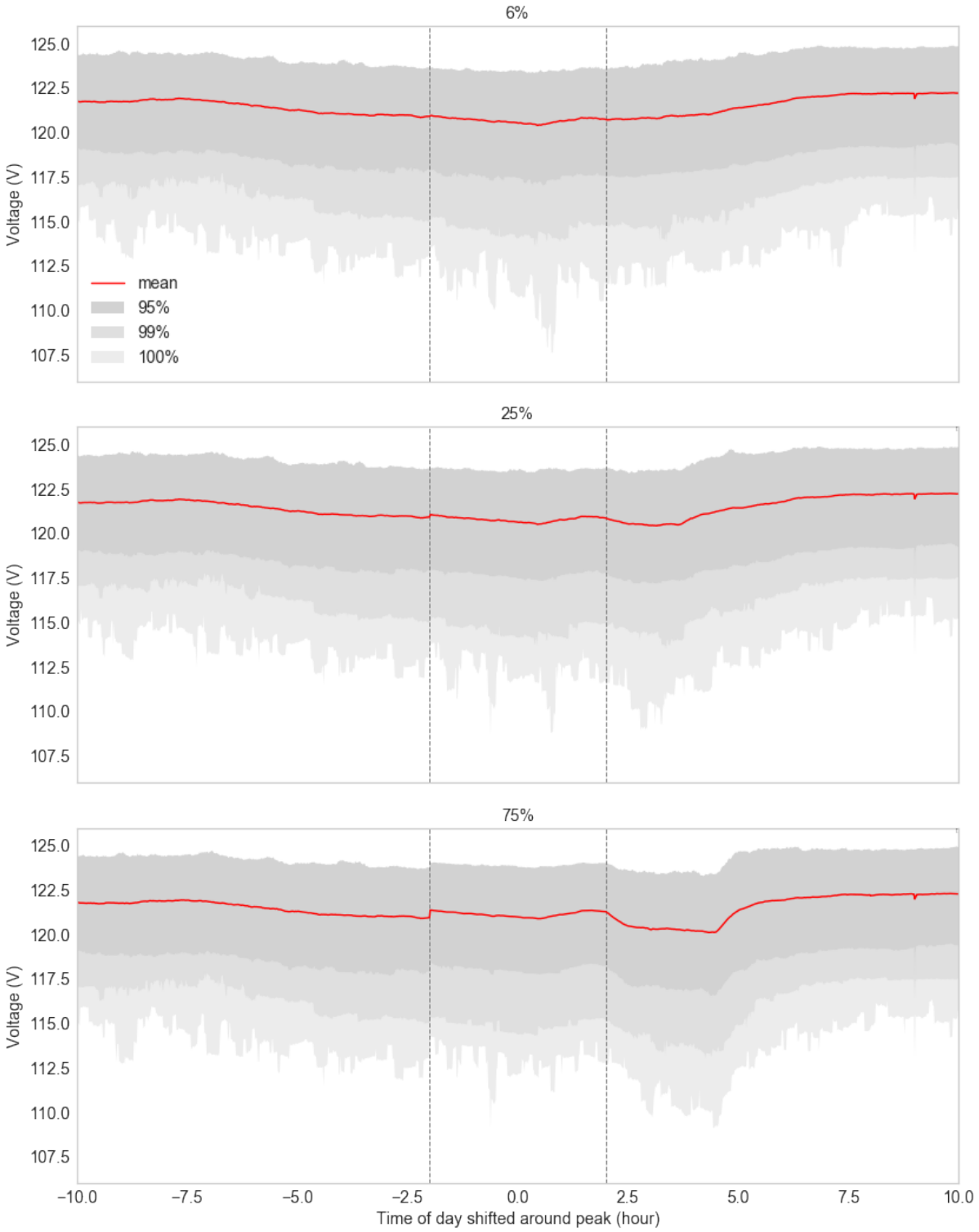

Figure 24: Feeder voltages on the 9G2 feeder during the summer time period with smooth control of EWHs at various levels: 6% (top); 25% (middle); 75% (bottom). The red line is the mean voltage, the gray area shows the range between minimum and maximum voltages with 95% of the meters falling in the darkest gray area and 99% falling in the medium and darkest gray areas.

The 9G2 feeder has a similar performance in the winter season at each penetration of controllable EWHs.

3.3 Impacts of Control Schemes on Water Heater Temperatures

The key tradeoff for using EWHs to support the grid was that, when EWHs were removed from service, households' hot water temperatures dropped and residents did not get the hot water they expected. This section summarizes impacts on hot water temperature under the two control schemes and the next section addresses the impacts on residents' comfort.

Figure 25 shows the differential between the water temperature and the set point for each of the EWHs on the ER-G51 feeder during the summer time period without any control other than keeping the water temperature within the deadband of +/- 5°F. The values were negative when the water temperature was lower than the setpoint and positive when the water temperature was greater than the setpoint. Temperatures within EWHs dropped due to two mechanisms: (1) hot water was used by residents and replaced with colder water, and (2) radiant, conduction, and convection losses. Under high demands for hot water, the temperature drop was observed to be up to 25°F even when the EWH was in service. Figure 25 shows that the average tank temperature was at the set point and that most of the EWHs were within a few degrees of the average. However, at any given time there were EWHs that were well below the set point because residents in those houses had used a lot of the water from their heater and were continuing to use hot water faster than the EWH could heat it.

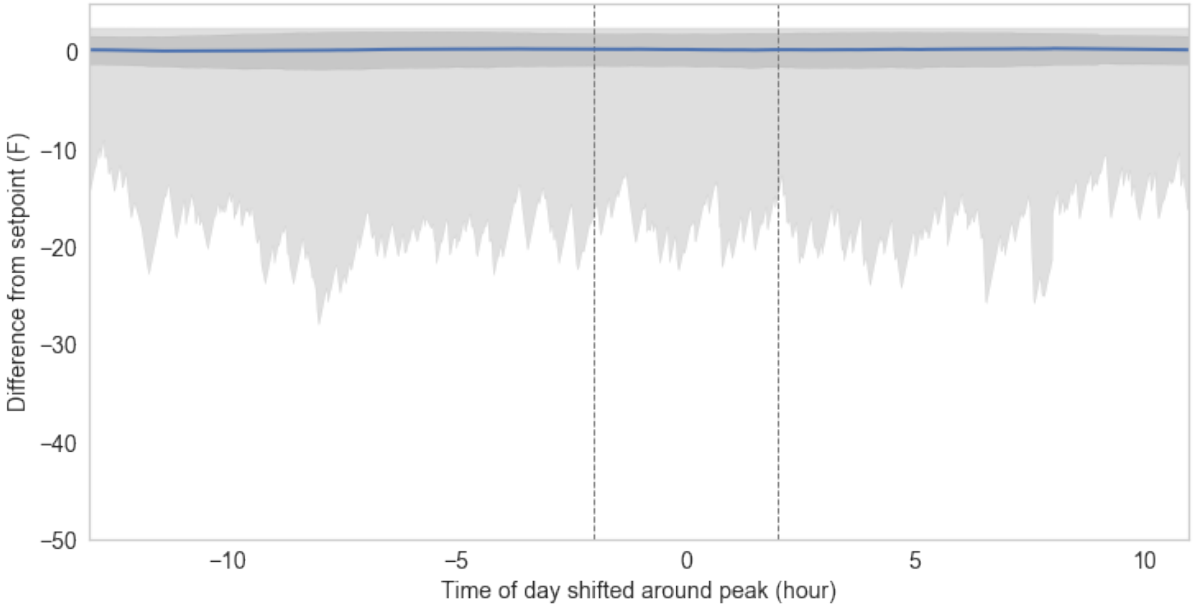

Figure 25: Differential between EWH set point temperature and the temperatures within the EWHs for houses on the ER-G51 feeder during the summer time period without any control. The blue line is the mean differential, the darker gray area shows an increase and decrease of one standard deviation, and the lighter gray area shows the extreme during each one-minute sampling period.

The impacts of the single-bucket control scheme on the differential between the EWH tank temperature and its setpoint are shown in Figure 26. The top, middle, and bottom images in that figure show the average, standard deviation and extent of the differentials on the ER-G51 feeder during the summer time period with 6%, 25%, and 75% of the EWHs under control, respectively. The average differential, its standard deviation, and the minimum temperature within the population dropped throughout the control period hitting minima at the time when EWHs were returned to service (at the end of the control period). However, the average did not drop too much; it was only 4°F lower than the setpoint at the end of the control period even with 75% of the EWHs being controlled. The lowest extreme differential dropped

during the first two hours of the control period and hit its lowest point in the middle of the peak control event. That trend indicates that some EWHs were available for all houses during the first two hours of the control period but at least one EWH had no hot water between that time and when the EWH were returned to service. The number of EWHs without hot water and the impacts on the residents is discussed in this report's next section.

Figure 27 shows the impacts of the smooth-control scheme on the differential between the hot water temperature and its setpoint. Like the single-bucket control scheme, the average differential, its standard deviation, and the minimum temperature within the population dropped throughout the control period, and the average differential was about 4°F lower than the setpoint at its lowest point. The main difference in the differential between the two control schemes was that the smooth-control scheme resulted in long periods where the lowest extreme temperature occurred after the peak control event. In addition, temperature differentials were greater than 30°F lower than the setpoint because many of the hot EWHs were not turned back on for 1-2 hours after the peak control event ended.

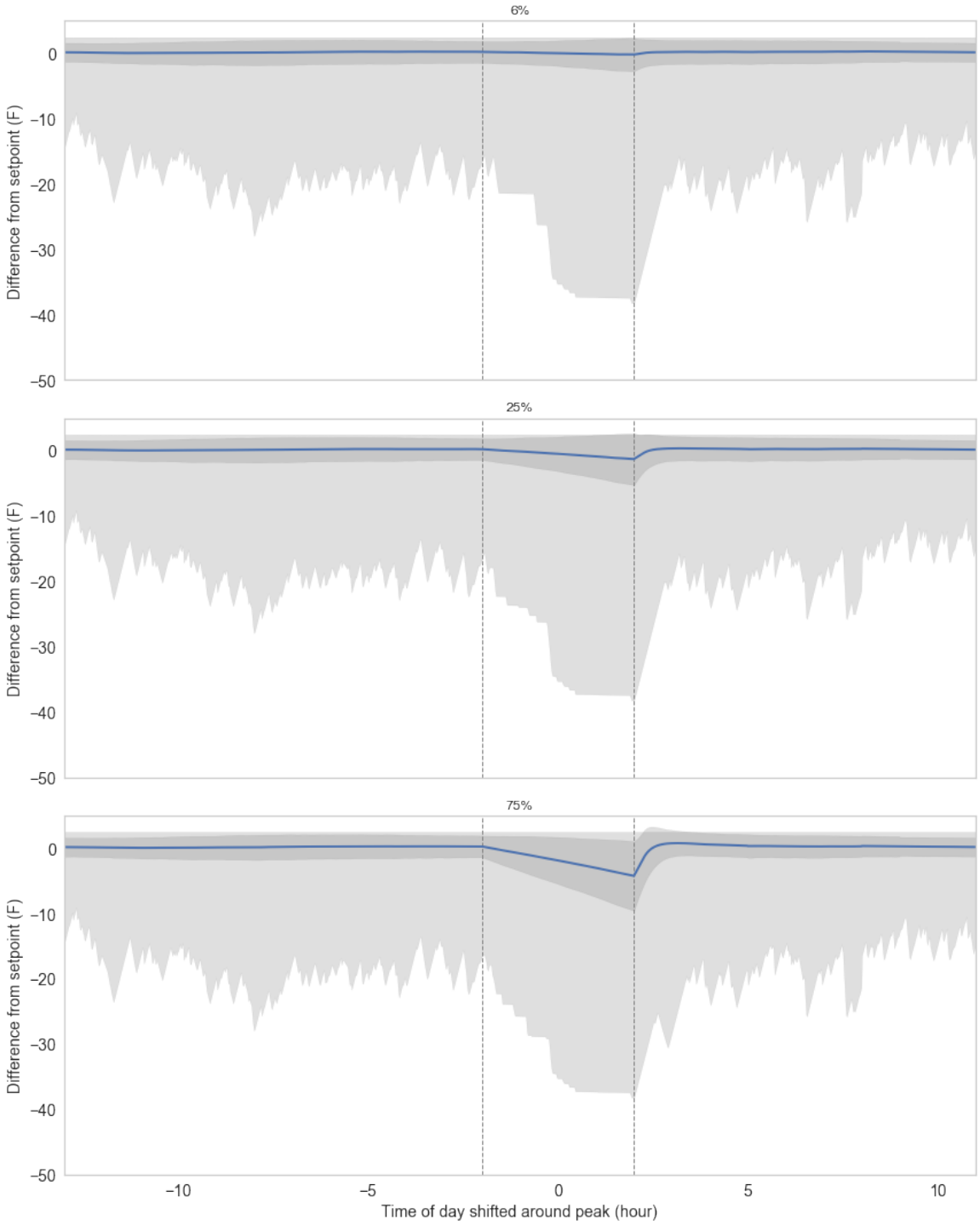

Figure 26: Differential between EWH set point temperature and the temperatures within the EWHs for houses on the ER-G51 feeder during the summer time period with single-bucket control of EWHs at various levels: 6% (top); 25% (middle); 75% (bottom). The blue line is the mean differential, the darker gray area shows an increase and decrease of one standard deviation, and the lighter gray area shows the extreme during each one-minute sampling period.

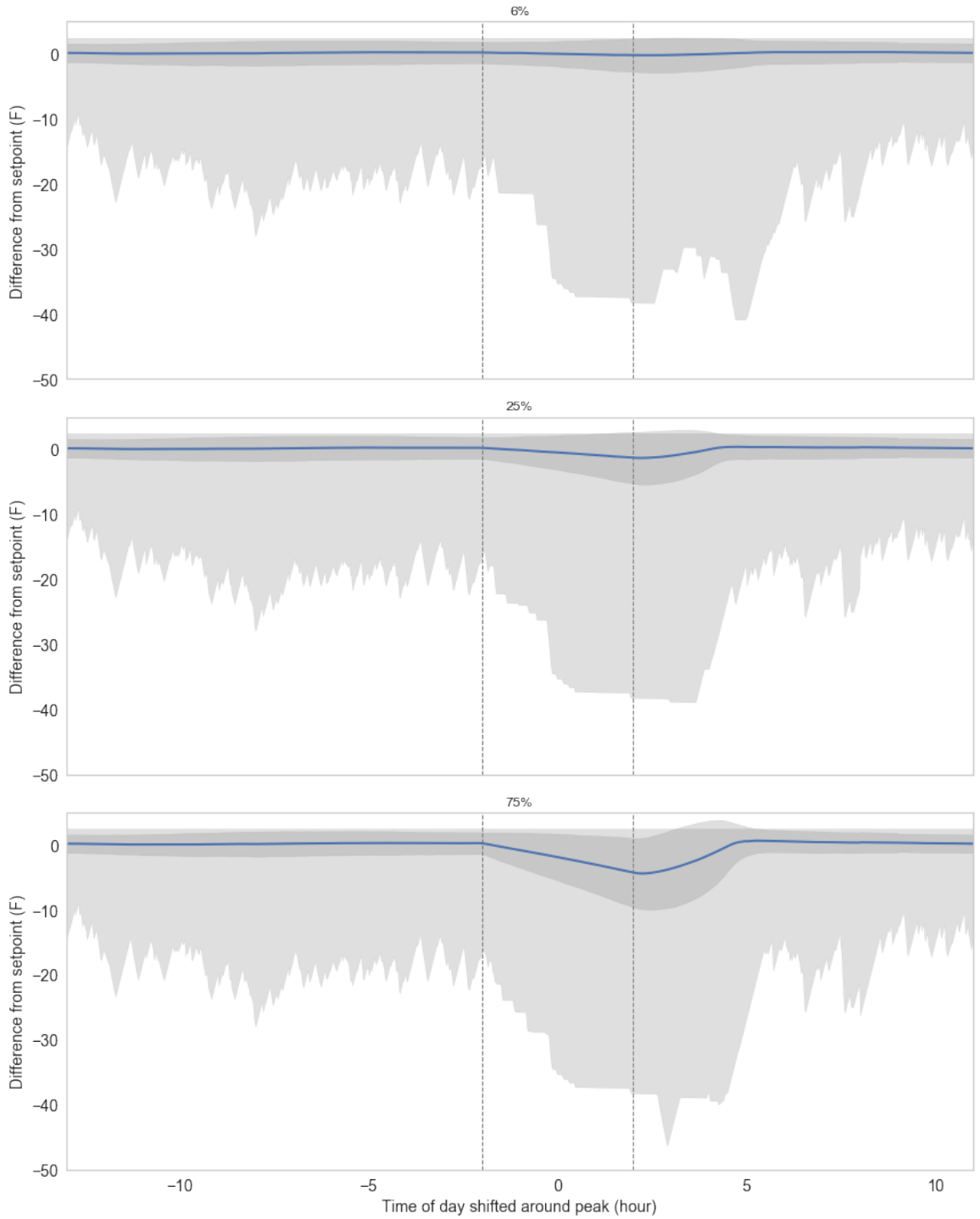

Figure 27: Differential between EWH set point temperature and the temperatures within the EWHs for houses on the ER-G51 feeder during the summer time period with smooth control of EWHs at various levels: 6% (top); 25% (middle); 75% (bottom). The blue line is the mean differential, the darker gray area shows an increase and decrease of one standard deviation, and the lighter gray area shows the extreme during each one-minute sampling period.

The differential between the EWH temperature and its set point are consistent between the two feeders and mostly consistent between seasons as Figure 28 shows for an example scenario. The average, average-minus-one standard deviation, and the low extreme differential all become slightly more negative during the winter season. The other control scheme and scenarios with different penetrations of controllable EWHs have the same patterns of EWH differential so they are not shown here.

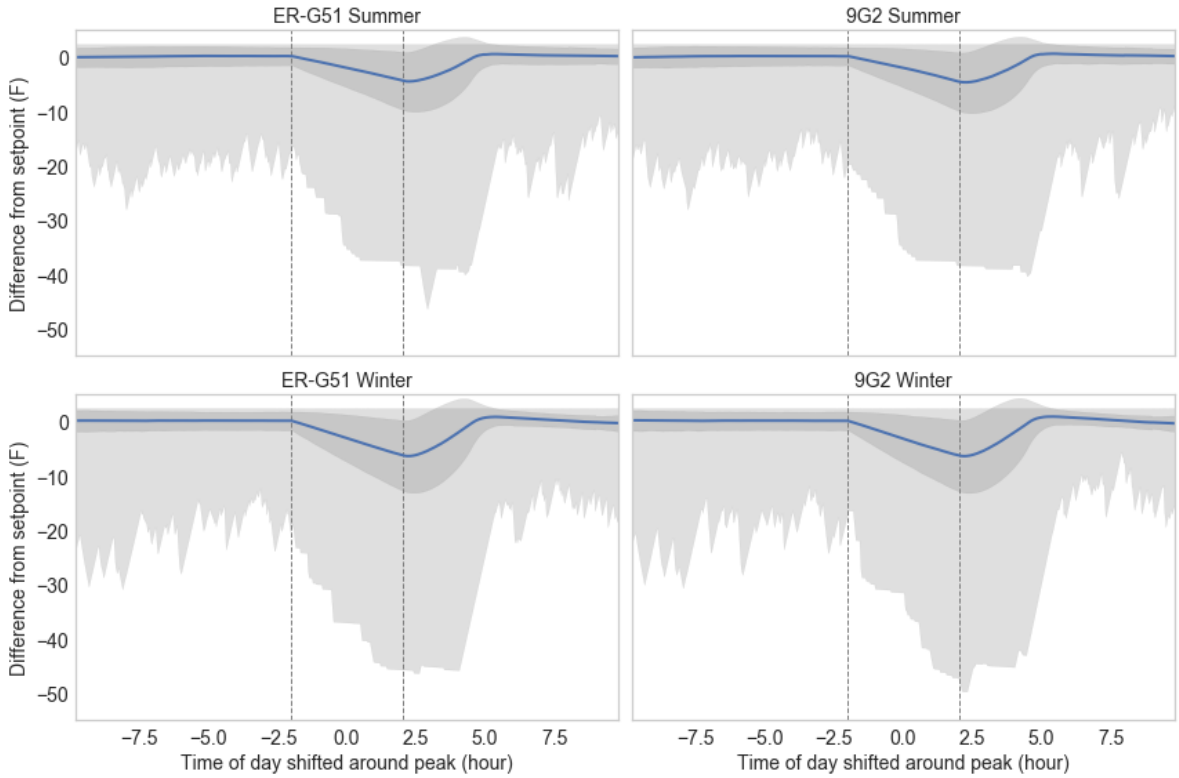

Figure 28: Comparison between EWH differentials from the set point at 75% penetration with the smooth-control scheme for the ER-G51 feeder (left) and the 9G2 feeder (right) during the summer (top) and winter (bottom) time periods

3.4 Impacts of Control Schemes on Water Comfort

Resident comfort depends upon getting hot water at a desired temperature when it is needed, so there are two factors involved: water temperature and demand for that water. We developed a metric that can identify uncomfortable customers as those whose hot water demand was greater than 0.4 gpm (e.g., a shower) when the hot water temperature was less than 110°F. Figure 29 shows the average percentage of customers in the summer on the ER-G51 feeder who were uncomfortable for each ten-minute period for both control schemes. Even when no control was exerted, a number of customers (less than 1%) were uncomfortable because they used up all the hot water in their EWHs but would have liked to use more. Increasing the percentage of EWHs taken out of service increased the number of uncomfortable customers during each 10-minute time period during the peak control event to a maximum of about 2.8% of the total customer base when 75% of the EWHs were controlled. The single-bucket control scheme limited the period during which customers were uncomfortable when compared to the smooth scheme because all the EWHs were returned to service at the same time instead of over a 2-3 hour period.

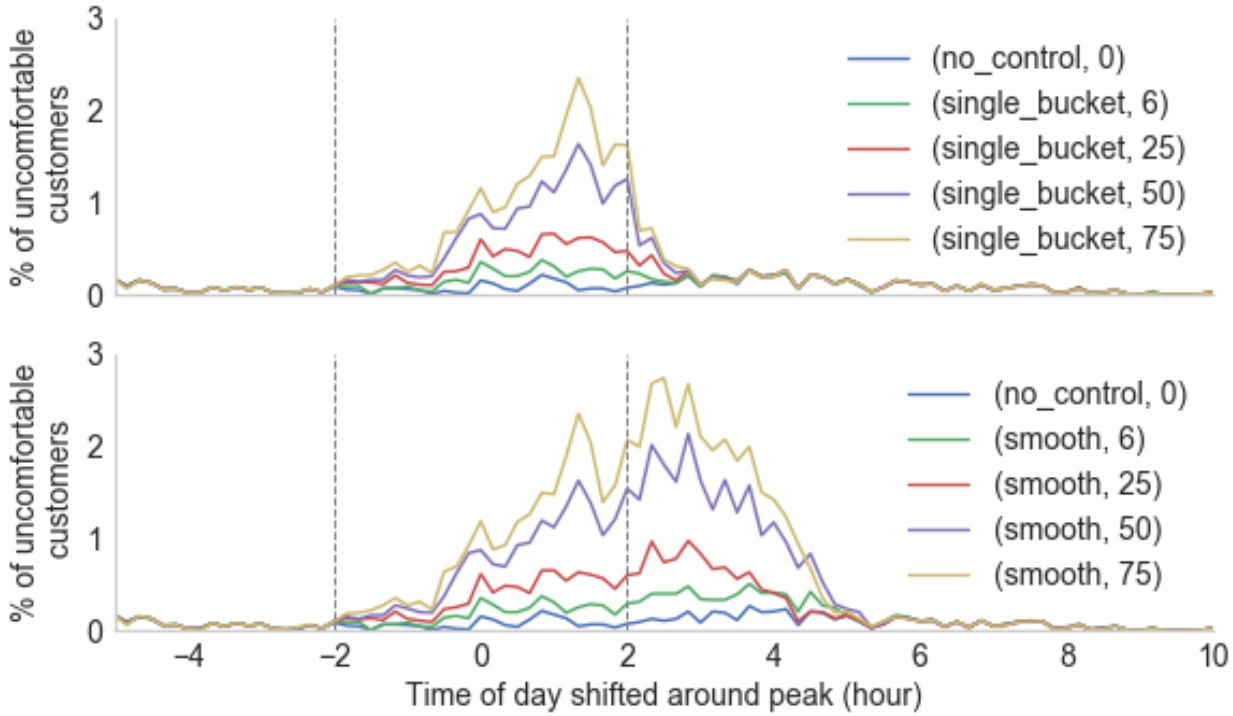

Figure 29: Percentage of uncomfortable customers during each ten-minute period on the ER-G51 feeder during the summer time period under no control and the single-bucket control scheme (top) and the smooth-control scheme (bottom).

Figure 30 shows the cumulative percentage of uncomfortable customers on the ER-G51 feeder during the summer time period under no control and each control scheme. The cumulative count starts at the beginning of the peak control event periods (i.e., 2 hours before the forecast peak time). Even with no control, approximately 1.8% of the customers had at least one period of discomfort before and during the 4-hour peak control event period and 3% up to and through the 12 hours shown in the figure. Increasing penetrations of controllable EWHs increased the cumulative number of customers with at least one uncomfortable period up to 5% before and during the peak control event period when 75% of the EWHs were being controlled under both control schemes. This is because the same EWHs were removed from service during the peak control event period under each. Under the single-bucket control, after the peak control event period the increase in uncomfortable customers matched that of the non-controlled simulations, indicating that a different set of customers were impacted after the peak control event than during the event. The number of customers with at least one uncomfortable period under the smooth-control scheme increased until all the EWHs were returned to service, nearly doubling the number that was impacted at the end of the peak control event period. Thus, the smooth-control scheme reduced the rebound and improved the voltage issues but increased the potential for complaints due to a lack of hot water.

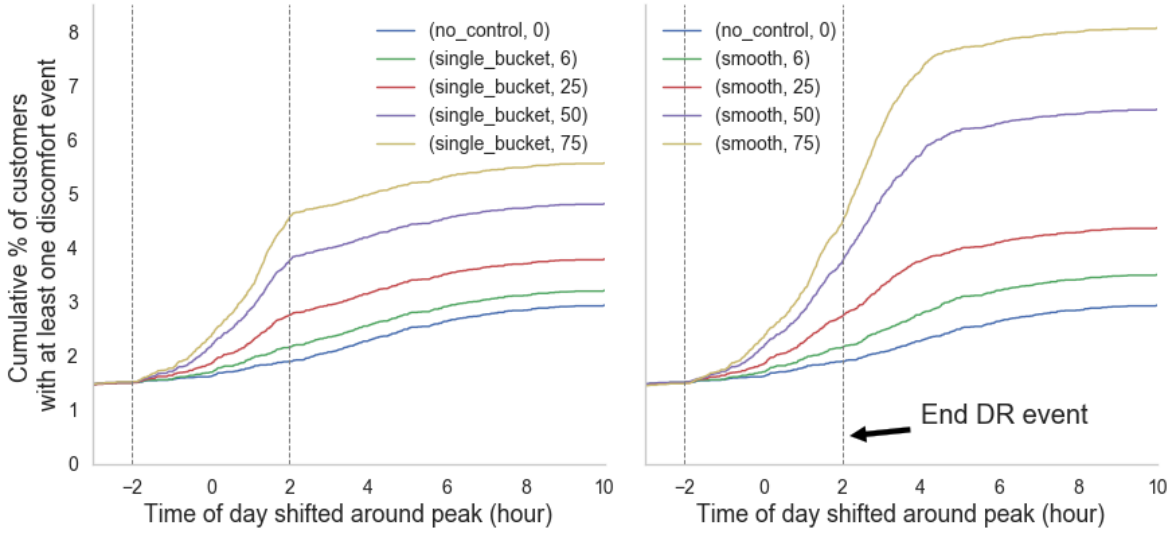

Figure 30: Percentage of customers with at least one discomfort (<110°F) 10-minute period after the beginning of the control period on the ER-G51 feeder during the summer time period under the single-bucket control scheme (left) and the smooth-control scheme (right).

Occupant hot water temperature threshold preference varies, but many customers feel discomfort between 105°F (Hendron-B) and 110°F (Wilson). The metric used for Figure 29 and Figure 30, is the most conservative discomfort metric—temperatures of 110°F and lower. Figure 31 shows the metric using 105°F as the criteria instead of 110°F. It shows that about 0.5% of customers experience an uncomfortable period each day when no control is enacted. At a 75% penetration of controllable EWHs, that number increases to approximately 1.5% during the peak control event time and to 3% over the 12-hour period shown under the smooth-control scheme.

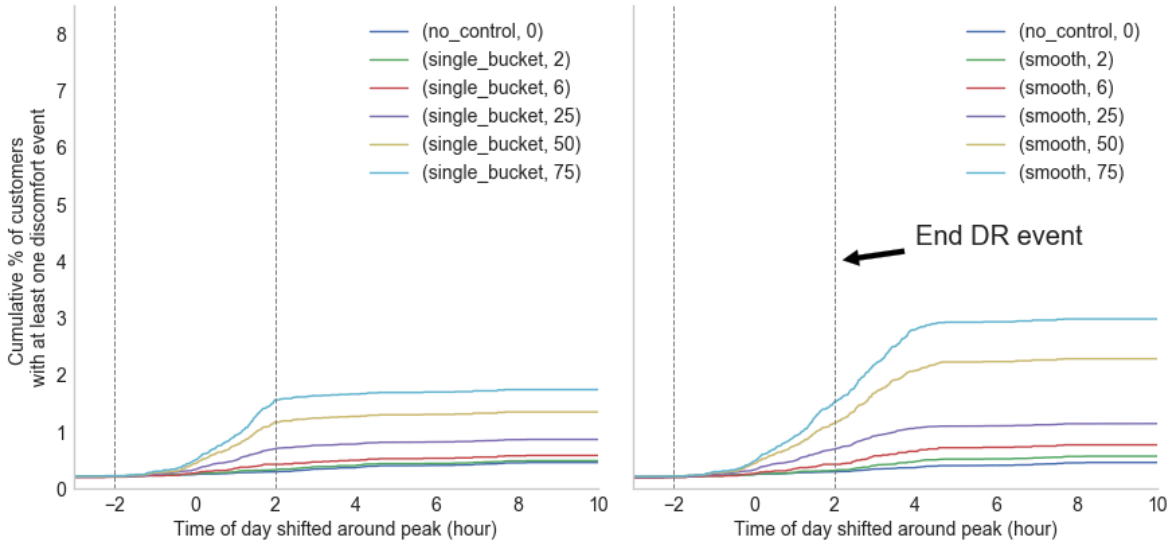

Figure 31: Percentage of uncomfortable customers with at least one discomfort (<105°F) 10-minute period after the beginning of the control period on the ER-G51 feeder during the summer time period under the single-bucket control scheme (left) and the smooth-control scheme (right).

Based on the data shown in Figure 30 and Figure 31, the percentage of customers who experienced at least one period of discomfort with their hot water system is shown in Table 7. However, even in the worst case scenario (75% penetration of controllable EWHs and the smooth-control scheme), only 3%–8% of the customers experienced at least a minute of discomfort during a day with a peak control event. Hence, 92%–97% of customers on the feeder will not realize they are impacted by the controls. Lower penetrations and the single bucket control scheme reduces the number of customers experiencing discomfort.

Table 7: Percentage of customers experiencing at least one 10-minute period when they are uncomfortable due to low water temperatures in any controlled day on the ER-G51 Feeder during the summer period (lower value indicates discomfort at 105°F and higher value at 110°F)

Number (%) of Controllable Water Heaters	Single-Bucket Control Scheme	Smooth-Control Scheme
0 (0%)	0.5% - 3%	
60 (6%)	0.6% - 3.2%	0.8% - 3.5%
250 (25%)	0.9% - 3.8%	1.2% - 4.4%
500 (50%)	1.4% - 4.9%	2.3% - 6.6%
750 (75%)	1.8% - 5.6%	3.0% - 8.1%

3.5 Potential Utility Cost Savings

The primary savings enabled by control schemes such as the ones in this report are reduced capacity charges. Capacity charges are the costs paid to the ISO to ensure that the ISO has sufficient generation and transmission capacity to provide energy at the peak times. They are location specific and are calculated based on the peak load over a time period—usually a year or a month. Capacity charges can be cut by decreasing the overall load through efficiency or by reducing the load at the time of the ISO peak (the strategy tested in this report). The objective of peak reduction DR programs is to reduce the load, thus reducing the capacity charge.

GMP pays two capacity charges [Hines]:

- A generation capacity charge of approximately $130/kW-year
- A transmission capacity charge of approximately $8/kW-month.

A key difference between the two is the time period over which they were effective. The generation capacity charge was for the highest load during a year and the transmission capacity charge is for the highest load during each month.

In Figure 32, we estimate the savings of control during a month. For the calculation, we combined the generation and transmission capacity charges into one value. Hence, we are considering only one month in the year and that the annual peak occurred in the month used in the evaluation. We also assumed that the control efforts would reduce the annual peak load and the peak load during the month by the average reduction in the peak load (as reported in Section 3.1). Thus, we estimated the total savings as $138/kW reduced from the peak. We report results for the winter because the peak load in the winter was higher

than it is in the summer. The assumption of $138/kW savings may be too optimistic if other days during the month and year have peak loads between the feeder's reduced peak and its original peak.

The rebound effect on load is also a key issue when considering savings. If the rebound causes a new, higher peak across the entire service territory, the peak may move to the time when the rebound occurs. A single feeder is unlikely to impact the ISO-NE peak; however, a large number of feeders with similar control and large rebounds (as seen with the single-bucket control scheme in Section 3.1) may increase the overall peak, thus increasing capacity charges. The rebound peak is not considered in these estimates.

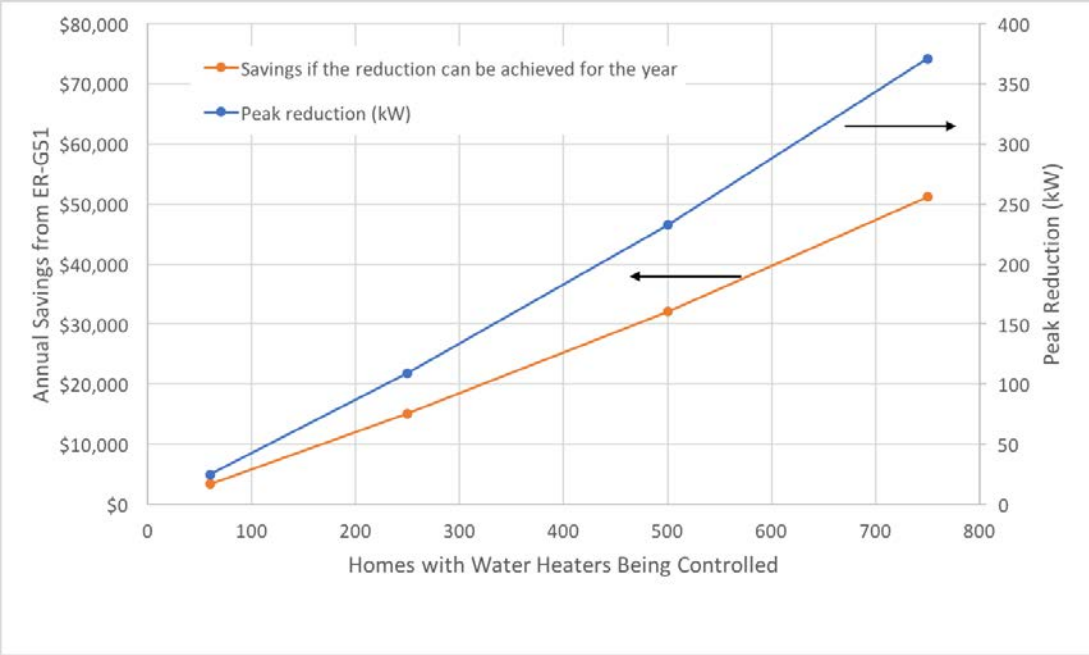

Figure 32: Potential reduction in peak load (right axis) and financial savings by cutting capacity charges (left axis) on the ER-G51 feeder during the winter time period

Table 8 and Table 9 show the potential capacity charge savings on each feeder assuming the control efforts would reduce the annual peak load and the peak load during the month by the average reduction (i.e., the total savings is reported as $138/kW reduced from the peak). Controllable EWHs on the ER-G51 feeder alone can reduce the capacity charge by up to $51,000 in a year and on the 9G2 feeder by $46,000. Additional mechanisms such as PV and batteries could reduce that charge more substantially.

Table 8: Potential Capacity Charge Savings on the ER-G51 Feeder

Number of Controllable Water Heaters	Season	PV Penetration	Battery Penetration	Peak Load Reduction (kW)	Potential Annual Savings ($/yr)
60 (6%)	Summer	0%	0%	6	$820
250 (25%)	Summer	0%	0%	67	$9,300
500 (50%)	Summer	0%	0%	150	$20,000
750 (75%)	Summer	0%	0%	250	$35,000
60 (6%)	Winter	0%	0%	25	$3,500
250 (25%)	Winter	0%	0%	110	$15,000
500 (50%)	Winter	0%	0%	230	$32,000
750 (75%)	Winter	0%	0%	370	$51,000
0	Summer	5%	0%	3 *	$500 *
250 (25%)	Summer	5%	0%	100 *	$14,000 *
0	Summer	25%	0%	110 *	$16,000 *
250 (25%)	Summer	25%	0%	200 *	$27,000 *
0	Summer	0%	25%	230	$32,000
250 (25%)	Summer	0%	25%	320	$45,000

* PV solar generation probably cannot be utilized to reduce peak loads because that peak reduction is dependent upon the irradiance during the peak time. However, over a two-week period during the summer, PV solar reduces the average peak during the key hours.

Table 9: Potential Capacity Charge Savings on the 9G2 Feeder

Number of Controllable Water Heaters	Season	PV Penetration	Battery Penetration	Peak Load Reduction (kW)	Potential Annual Savings ($/yr)
48 (6%)	Summer	0%	0%	17	$2,300
200 (25%)	Summer	0%	0%	75	$10,000
400 (50%)	Summer	0%	0%	130	$18,000
600 (75%)	Summer	0%	0%	210	$28,000
48 (6%)	Winter	0%	0%	15	$2,100
200 (25%)	Winter	0%	0%	84	$12,000
400 (50%)	Winter	0%	0%	200	$27,000
600 (75%)	Winter	0%	0%	330	$46,000

4.0 Conclusions

The purpose of this analysis was to evaluate and quantify potential benefits and impacts of two control schemes for centrally controllable EWHs on two GMP feeders. The control schemes were designed with several objectives. The first was to reduce the load during peak load times when capacity charges are the primary costs. The second was to mitigate DR rebound to avoid new peak load times and high ramp rates. The final objective was to minimize customers' discomfort—lack of hot water when it was needed.

We tested several different penetrations of controllable EWHs: 0% (to set a baseline), 6% (to match the current penetration on the ER-G51 feeder), 25%, 50%, and 75%. In addition, we compared feeder performance with and without batteries and PV to provide a comparison of options and identify potential synergies.

One key challenge for this type of simulation was the necessary data requirements. We did not have customer-specific data on the feeder so we populated the feeder with census data for house size, age, and occupancy characteristics. Since the focus of this analysis was on EWHs, hot-water-draw characteristics were critical for the analysis; however, those characteristics were not available so we used literature data to estimate the draw characteristics.

The simulation found that hot water draw rates, which is a key driver for EWH power use, do not always match up with peak load times, so EWHs may not be the best option for load shedding (i.e., because water draw is low during the hours when peak load times occur, shedding other loads may provide a larger load reduction).

Figure 33 showed that the control schemes could reduce up to 25% of the peak load on a feeder but that higher peak load reductions resulted in increased rebound peaks. That peak load reduction on the ER-G51 feeder alone was estimated to reduce the capacity charge by up to $51,000 in a year and on the 9G2 feeder by $46,000 a year. Additional mechanisms such as PV and batteries could reduce that charge more substantially.

The smooth-control scheme was more effective than the single-bucket approach at limiting the rebound. Under the single bucket control scheme, the rebound was up to 175% higher than the original peak. The smooth control scheme mitigated that effect with no rebounds greater than 40% higher than the original peak. At low controllable EWH penetrations (6%), the rebound peak was lower than the uncontrolled peak.

By reducing the size of the rebound, the smooth-control scheme reduced the frequency of voltages less than 114 thus improving electricity service to the customers and likely reducing costs to maintain the distribution feeder.

Rebounds were smaller in the winter than in the summer.

During the summer, a combination of PV solar and EWH control can reduce the peak more than either alone as long as the solar irradiance is high during the peak control time; however, PV solar does not benefit the rebound as much because the rebound occurs at the same time PV generation goes down due to the setting of the sun.

Batteries alone reduced the peak load by 21% during the peak control event. The rebound they introduced was late at night when the sum of the battery charging, ZIP, and EWH loads was lower than during the day. Including the EWH control could reduce the peak load by an additional 5% but introduced rebounds

like those when no battery was present; however, the rebound peak for the single-bucket control scheme was not as high as without a battery because the battery was continuing to discharge for the first 30 minutes after the peak control event—the time when the single-bucket rebound peak was highest. A load spike occurs when batteries stop discharging at that time.

Figure 33 also shows that increased penetrations of controllable EWHs increased the number of customers experiencing at least one minute of discomfort during an average day (bottom image). Even without centralized EWH DR control, approximately 3% of customers daily experienced a minute where hot water temperature was below 110°F because the EWH reservoir was drained of hot water and their draw exceeded the EWH's capacity to heat additional water to the expected level. Increasing penetration of controllable EWHs increased the number of customers with a discomfort minute to more than 120 customers on the on the ER-G51 feeder (12% of the customers under the smooth control scheme in the worst case).

The smooth-control scheme resulted in 0.3%-2.5% more customers who experienced discomfort on an average day with a peak control event than under the single-bucket control scheme because the EWH for some customers is out of service for longer periods of time.

The smooth control scheme reduced the rebound but has the potential to increase the number of complaints due to a lack of hot water. However, even in the worst case scenario (75% penetration of controllable EWHs and the smooth-control scheme), only 3%–8% of the customers experienced at least 1 minute of discomfort during a day with a peak control event. Hence 92%–97% of customers on the feeder did not realize they were impacted by the control scheme. Lower penetrations and the single-bucket control scheme reduced the number of customers experiencing discomfort.

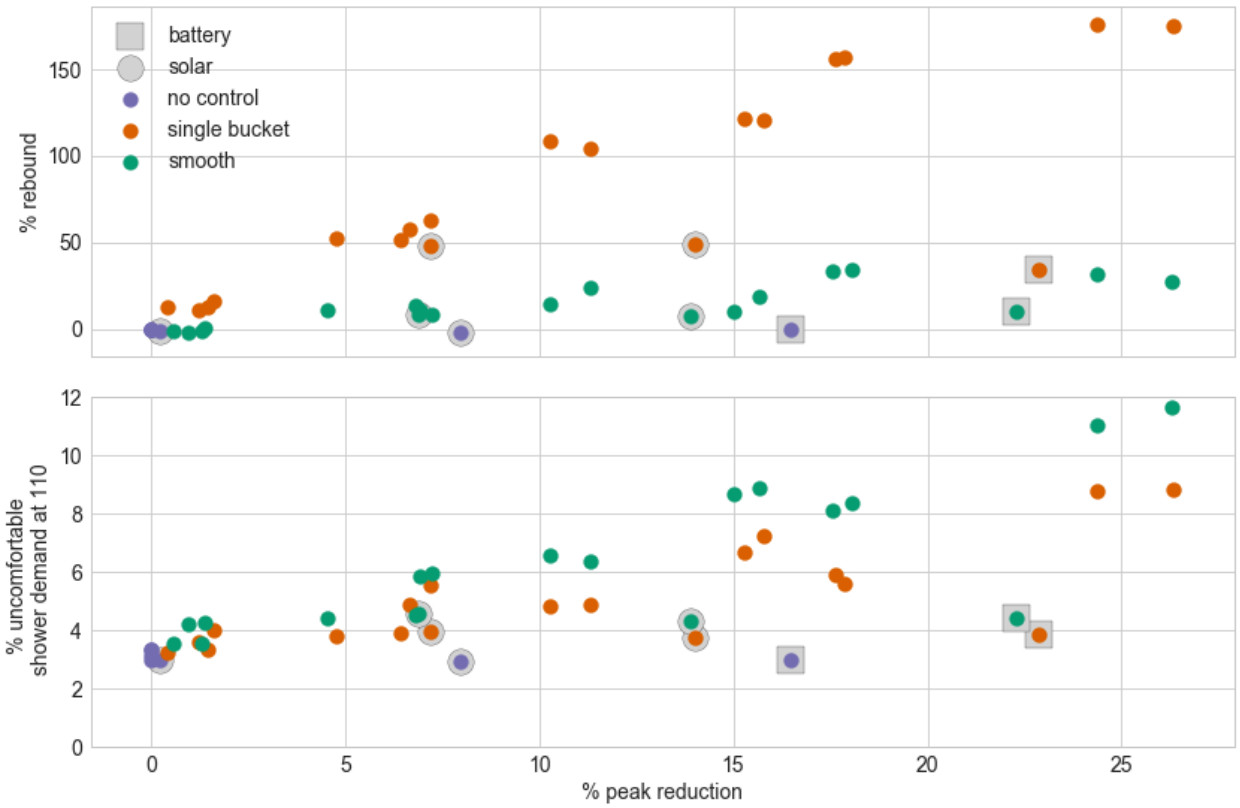

Figure 33: Peak load reductions and corresponding rebounds (top) and average number of customers with at least one minute without hot water in a day (bottom) for all simulations performed. Dot color indicates DR control scheme and outline shape indicates whether batteries or PV solar were included in simulations.

5.0 Suggested Improvements to Simulation and Control Strategy

5.1 Other Considerations for Control

5.1.1 Alternatives for Managing Capacity Charges While Limiting Impacts on Comfort

In this analysis, we considered two control schemes that manage capacity charges. A key parameter for both control schemes was a 4-hour window around the peak load time. EWHs were removed from service 2 hours before the forecast peak load and not returned to service until 2 hours after the forecast peak. If the forecast were improved, that window could be shortened. Shortening could reduce the amount of time during which water would be drawn without the EWH being able to heat water from the main. Therefore, the shorter peak control event has the potential to reduce the cumulative number of uncomfortable customers.

An alternative is to turn EWHs back on when / if they reach a minimum temperature (say 110°F), which is likely to reduce the number of uncomfortable customers but could also reduce the peak savings unless additional customers are added to the program. One challenge with this alternative scheme is that it requires communication of water temperature to the centralized control system or inclusion of local controls that allow the system to return to service during the peak control event. Each of these options require more sophisticated control and communications.

A slightly modified version of the scheme is to keep all the EWH out of service during the entire peak control event period but order how they are returned to service by turning on the EWH with the coldest water first and reviewing the temperature of each EWH each time more are returned to service. This allows the EWHs with the coldest water to be identified and returned to service first. This scheme also requires communication of the EWH temperature.

A combined battery-EWH control scheme could likely be developed such that the battery would both reduce the peak during the peak control event and limit the rebound. That strategy could be designed so that battery discharge keeps the net load on the feeder below a certain point during the peak control event and then return EWHs to service at a rate faster than the one simulated in this project but slow enough to limit additional load to be less than the battery discharge rate. In addition, use of batteries alone to manage peak may be sufficient on most days so that control of EWHs is only needed a few days a year.

5.1.2 Alternative Control Objectives: Managing Ramp Rates at High PV Penetrations

The integration of solar PV systems on the electric grid presents complications for the utility. Locations where there is a high penetration of PV require operators to react quickly to large changes in the net load caused by the PV generation variability. The net load is the difference between the load and the PV generation as shown in Figure 34. The increase in demand coupled with the rapid reduction in solar power generation as the sun goes down can increase the challenge of balancing load and generation on the electric grid. This situation may require the deployment of an expensive generation station to rapidly come online and accommodate the load. EWHs have the potential to mitigate this issue by synchronizing their charging with the solar production (Jones).

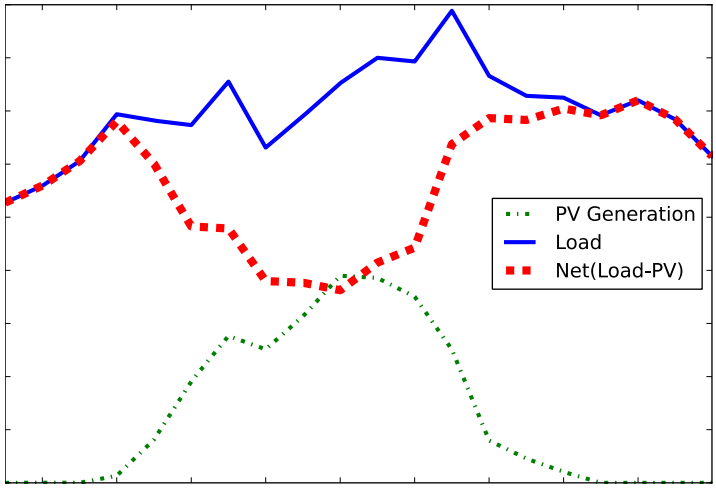

Figure 34: The net load is the difference between the load and the PV generation. The net load has a large ramp rate at the end of the day when the sun sets and demand increases. The change may require utility operators to turn on expensive generation stations.

EWHs can help mitigate ramp rate increases at higher PV penetrations by implementing a dynamic setpoint control system that can synchronize EWHs load with the solar power production and simultaneously maintain occupant comfort. Typical systems use a static setpoint control strategy. The setpoint temperature is the reference temperature that is compared with the actual water temperature to determine the control of the heating element inside the EWH tanks. If the water temperature (T_{water}) is less than the setpoint temperature (T_{sp}) by more than 2.7˚C then the heating element is turned on, as shown in Equation 3 (the simulations reported in this document have an almost identical range of +/- 5°F). In this experiment, we tested the viability of dynamic setpoint implemented a nonlinear function that is defined by Equation 4:

$$\text{Heating Element} = \begin{cases} On, if\ T_{water} < T_{sp} - 2.7^{\circ}C \\ Off, otherwise \end{cases} \quad (3)$$

$$T_{sp} = 12(E/1300)^3 + 45 \quad (4)$$

Where E is the measured irradiance (W/m^2), 1,300 was used to normalize the irradiance value, 12 is a multiplier, and 45°C is the minimum setpoint temperature. A maximum setpoint can also be set to prevent potential injury due to scalding and potential equipment damage.

A preliminary simulation was run to test this dynamic control strategy in a Python simulation environment that emulated a total of 2,900 EHWs on a single feeder. The simulation included multizone models of the water heaters unlike the other simulations discussed in this report. The simulated feeder had a maximum load of 10 MW and a PV system that reached a maximum of 3.8 MW in the middle of a summer day.

The typical EWH operations that used a static setpoint controller for all the EWHs produced a peak of about 2 MW for the EWHs alone, as shown in Figure 35. The dynamic setpoint control algorithm was applied to 33% of the EWHs and was able to alter their charging. The change in operations increased the peak to about 5 MW and synchronized the load with the PV generation.

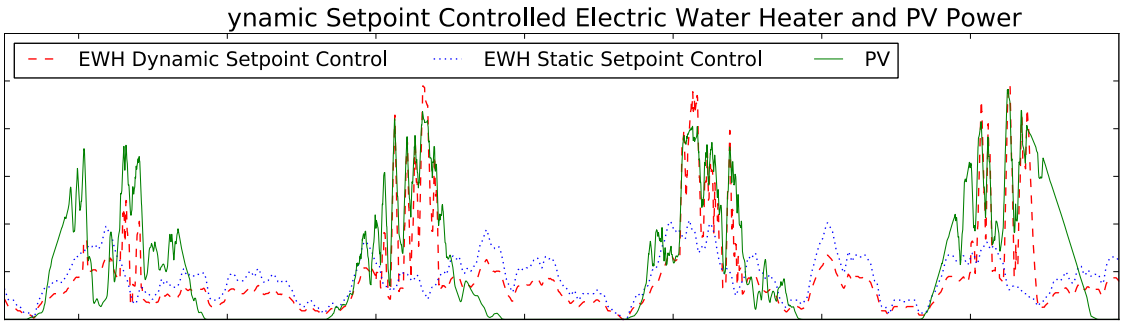

Figure 35: The static setpoint controllable EWHs did not match well with the PV production profile. The dynamic setpoint controlled approach applied to about 33% of the 2,900 EWHs' synchronized consumption with the PV generation over a 4-day period.

The control of the 33% or 867 of the 2,900 EWHs affected the net load by increasing the demand during the day and decreasing it during the night. This result was computed by first subtracting the baseline EWH demand from the simulated net load and then adding the results from the dynamically controlled EWH simulation. The new load profile, shown in Figure 36, reduced the magnitude of the load reductions and decreased the magnitude of the rebounds. The approach also eliminated the large ramp rate that had occurred between 14:00 and 15:00.

The simulation effort also calculated the average temperature at the top and bottom of the dynamically controlled hot water tanks. During the same 4-day period plotted in Figure 35 the average temperature at the top of the tank did not drop below 50°C. Additionally, the bottom temperature did not drop below 47.5°C. In conclusion, the average temperature for the EWHs can continue to provide desired hot water to occupants while simultaneously synchronizing the PV generation.

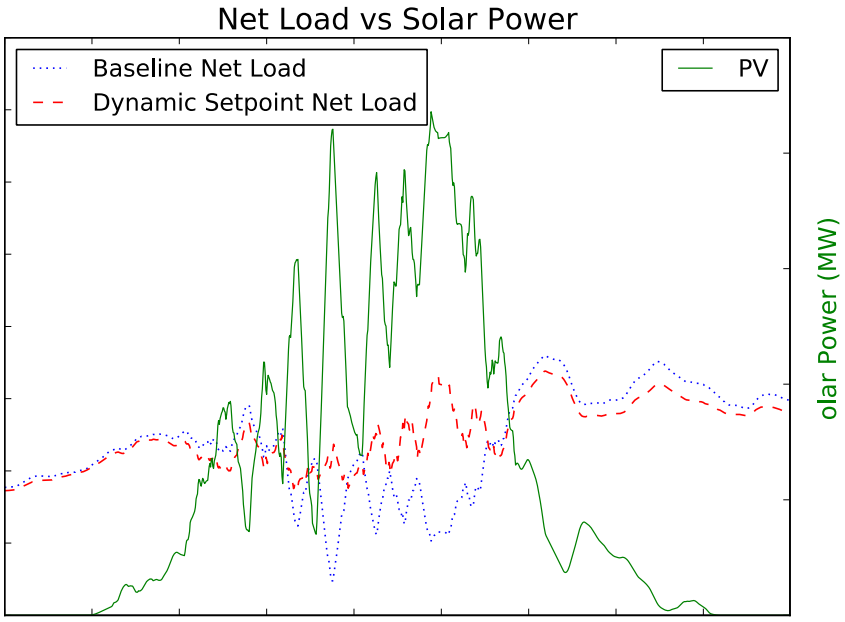

Figure 36: The solar irradiance dependent setpoint algorithm was able to fill in the net load valley created by the PV production and smooth the variability slightly.

5.2 Model Validation

The primary validation challenge was that the capacity charges were for the full region, not just for the feeders analyzed. The impacts of the control schemes analyzed were only estimated for the ER-G51 and 9G2 feeders; however, since the load shape of the region used for the capacity charge was not available for this analysis, the overall impacts (both positive and negative) of the control schemes were difficult to estimate. Specifically, the impacts of the load rebound when EWHs were returned to service may not matter if the other loads in the region have gone down sufficiently to keep the peak load during the rebound under the highest peak of the region.

A second challenge was validating models against load data because of a lack of information about the houses and their water use. In addition, water use data are needed at a high frequency (e.g., 1 minute) because hour-long averages are insufficient for energy use calculations. To accurately model feeder performance, especially voltage, accurate loads are needed. In addition, field measurements of voltage are needed to validate the model. On residential feeders, those loads are dependent primarily upon utilization of appliances. In this analysis, the key focus is EWHs because they are a high fraction of load in Vermont (unlike other locations where air conditioners are the primary loads due to different weather patterns and/or use of gas to heat water). Water use data are almost never measured so estimates needed to be developed based on known utilization and census data on house size. The census data are on the full population so loads in specific locations were not validated against the AMI data for those locations.

5.3 Other Considerations

Another consideration for peak load management is more efficient appliances. As the population of appliances becomes more efficient, the peak load is likely to go down unless the population grows at a greater rate or additional loads overcome the reduction (e.g., increase in air conditioner loads). The subsequent challenge created by efficiency improvements is that additional loads will need to be removed

from service to achieve the same peak load reduction. If efficient water heaters (e.g., heat pump water heaters) replace the current stock, a higher percentage will need to participate in the peak load reduction program or more options for peak load reduction will need to be included to achieve the same effect.

If batteries are on in many of the houses, they can be operated in alternative ways that reduce the rebounds. In this study, we simulated battery discharge at its full rate during the 5 hours they required to for full discharge. If the overall feeder load can be tracked, discharge rates can potentially be controlled to meet a specific target during the peak times and then be used at maximum rate to minimize rebound after the peak control event ends.

6.0 References

American National Standards Institute. "American National Standard For Electric Power Systems and Equipment—Voltage Ratings (60 Hertz)," ANSI C84.1-2011 Revision of ANSI C84.1-2006. (December 2006). https://www.nema.org/Standards/ComplimentaryDocuments/Contents-and-Scope-ANSI-C84-1-2011.pdf

Chassin, D. P., Fuller, J. C., and Djilali, N. "GridLAB-D: An agent-based simulation framework for smart grids," *J. Appl. Math.*, 2014.

Electric Power Research Institute. "OpenDSS COM Documentation Circuit Class Interface," September 26, 2013.

Green Mountain Power. "Off-Peak Water Heating Rate Schedule Company Designation 3" VPSB 9. First Revised . October 1, 2016 https://www.greenmountainpower.com/wp-content/uploads/2016/09/Rate-3-Off-Peak-Water-Heating-10.1.16.pdf (Green Mountain Power)

Grid Modernization Laboratory Consortium "DOE Grid Modernization Laboratory Consortium (GMLC) – Awards" https://energy.gov/under-secretary-science-and-energy/doe-grid-modernization-laboratory-consortium-gmlc-awards. Accessed October 27, 2017.

Hendron, R., Burch, J., Barker, G. "Tool for Generating Realistic Residential Hot Water Event Schedules," Presented at the SimBuild 2010 Conference, New York, NY, August 15-19, 2010. https://www.nrel.gov/docs/fy10osti/47685.pdf (Hendron-A)

Hendron, R., Engebrecht, C. "Building America Research Benchmark Definition Updated December 2009," NREL Technical Report, NREL/TP-550-47246. January 2010. https://www.nrel.gov/docs/fy10osti/47246.pdf (Hendron-B)

Hines, P. Personal communication about capacity charge in Vermont. September 13, 2017.

Jones, C. B., Lunacek, M., Lave, M., Johnson, J., and Broderick, R. "Dynamic Setpoint Control of Electric Water Heater Tanks for Increased Integration of Solar Photovoltaic Systems," 44th Photovoltaic Specialists Conference (PVSC), Washington D.C.,USA, 2017.

Mittal, S., Ruth, M., Pratt, A., Lunacek, M., Krishnamurthy, D., Jones, W. (2015) "A System-of-Systems Approach for Integration Energy Modeling and Simulation," Summer Computer Simulation Conference, Chicago, IL, July 26-29, 2015. http://www.nrel.gov/docs/fy15osti/64045.pdf

Ruth, M., Pratt, A., Lunacek, M., Mittal, S., Jones, W., and Wu, H. "Effects of House Energy Management Systems on Distribution Utilities and Feeders Under Various Market Structures," presented at the 23rd International Conference on Electricity Distribution (CIRED), Lyons, France, 2015.

Sandia National Laboratories, "Regional Test Centers for Solar Technologies" https://rtc.sandia.gov (Accessed October 2017)

U.S. Census Bureau, “Community Facts”
https://factfinder.census.gov/faces/nav/jsf/pages/community_facts.xhtml (Accessed September 2017)

Wilson, E., Engebrecht Metzger, C., Horowitz, S., Hendron, R. “2014 Building America House Simulation Protocols” NREL Technical Report, NREL/TP-5500-60988. March 2014.
https://energy.gov/sites/prod/files/2014/03/f13/house_simulation_protocols_2014.pdf

http://gridmodernization.labworks.org/